



**HAL**  
open science

## **A promising location in Patagonia for paleoclimate and paleoenvironmental reconstructions revealed by a shallow firn core from Monte San Valentín (Northern Patagonia Icefield, Chile)**

Françoise Vimeux, Martine de Angelis, Patrick Ginot, Olivier Magand, Gino Casassa, Bernard Pouyaud, Sonia Falourd, Sigfus Johnsen

### ► **To cite this version:**

Françoise Vimeux, Martine de Angelis, Patrick Ginot, Olivier Magand, Gino Casassa, et al.. A promising location in Patagonia for paleoclimate and paleoenvironmental reconstructions revealed by a shallow firn core from Monte San Valentín (Northern Patagonia Icefield, Chile). *Journal of Geophysical Research: Atmospheres*, 2008, 113 (D16118), 1 à 20 p. 10.1029/2007JD009502 . insu-00381108

**HAL Id: insu-00381108**

**<https://insu.hal.science/insu-00381108>**

Submitted on 28 Oct 2020

**HAL** is a multi-disciplinary open access archive for the deposit and dissemination of scientific research documents, whether they are published or not. The documents may come from teaching and research institutions in France or abroad, or from public or private research centers.

L'archive ouverte pluridisciplinaire **HAL**, est destinée au dépôt et à la diffusion de documents scientifiques de niveau recherche, publiés ou non, émanant des établissements d'enseignement et de recherche français ou étrangers, des laboratoires publics ou privés.

## A promising location in Patagonia for paleoclimate and paleoenvironmental reconstructions revealed by a shallow firn core from Monte San Valentín (Northern Patagonia Icefield, Chile)

Françoise Vimeux,<sup>1,2</sup> Martine de Angelis,<sup>3</sup> Patrick Ginot,<sup>1,3</sup> Olivier Magand,<sup>3</sup> Gino Casassa,<sup>4</sup> Bernard Pouyaud,<sup>1</sup> Sonia Falourd,<sup>2</sup> and Sigfus Johnsen<sup>5</sup>

Received 16 October 2007; revised 16 April 2008; accepted 8 May 2008; published 28 August 2008.

[1] The study of past climate variability from ice core investigations has been largely developed both in polar areas over the past decades and, more recently, in tropical regions, specifically along the South American Andes between 0° and 20°S. However a large gap still remains at mid-latitudes in the Southern Hemisphere. In this framework, a 15.3-m long shallow firn core has been extracted in March 2005 from the summit plateau of Monte San Valentín (3747 m, 46°35'S, 73°19'W) in the Northern Patagonia Icefield to test its potential for paleoclimate and paleoenvironmental reconstructions. The firn temperature is  $-11.9^{\circ}\text{C}$  at 10-m depth allowing to expect well preserved both chemical and isotopic signals, unperturbed by water percolation. The dating of the core, on the basis of a multi-proxy approach combining annual layer counting and radionuclide measurements, shows that past environment and climate can be reconstructed back to the mid-1960s. A mean annual snow accumulation rate of  $36 \pm 3 \text{ cm year}^{-1}$  (i.e.,  $19 \pm 2 \text{ g cm}^{-2} \text{ year}^{-1}$ ) is inferred, with a snow density varying between 0.35 and  $0.6 \text{ g cm}^{-3}$ , which is much lower than accumulation rates previously reported in Patagonia at lower elevations. Here, we present and discuss high-resolution profiles of the isotopic composition of the snow and selected chemical markers. These data provide original information on environmental conditions prevailing over Southern Patagonia in terms of air masses trajectories and origins and biogeochemical reservoirs. Our main conclusion is that the San Valentín site is not only influenced by air masses originating from the southern Pacific and directly transported by the prevailing west winds but also by inputs from South American continental sources from the E–NE, sometimes mixed with circumpolar aged air masses, the relative influence of these two very distinct source areas changing at the interannual timescale. Thus this site should offer a wealth of information regarding (South) Pacific, Argentinian NE–E areas and Antarctic climate variability.

**Citation:** Vimeux, F., M. de Angelis, P. Ginot, O. Magand, G. Casassa, B. Pouyaud, S. Falourd, and S. Johnsen (2008), A promising location in Patagonia for paleoclimate and paleoenvironmental reconstructions revealed by a shallow firn core from Monte San Valentín (Northern Patagonia Icefield, Chile), *J. Geophys. Res.*, 113, D16118, doi:10.1029/2007JD009502.

### 1. Introduction

#### 1.1. Background

[2] Antarctic ice cores analyses have been providing a wealth of detailed paleoclimate and paleoenvironmental information for more than 40 years [*EPICA community members*, 2004; *Wolff et al.*, 2006 for the most recent

examples]. Ice core investigations based on water stable isotopes and insoluble dust measurements have also been conducted in tropical regions, mainly along the South American Andes from the equator to about 20°S, allowing us to access to past tropical climate variability back to the last glacial maximum [see for instance *Ramirez et al.*, 2003; *Thompson et al.*, 2000 and 2003]. However a large gap still exists at mid-latitudes in South America, along the Equator-Pole transect. It is necessary to document the main features of the climate in this region, potentially impacted by numerous interannual to decadal large-scale phenomena rooted both in the tropical oceans as ENSO (El Niño Southern Oscillation, dominant mode of interannual tropical variability) [*Garreaud et al.*, 2008] and in high-latitudes as AAO (Antarctic Annular Oscillation or Southern Hemisphere Annular Mode controlled by the near-stationary wave associated with the sub-Antarctic westerlies) [*Gillett*

<sup>1</sup>IRD, Institut de Recherche pour le Développement, UR Great Ice, France.

<sup>2</sup>IPSL/LSCE, Laboratoire des Sciences du Climat et de l'Environnement, UMR CEA-CNRS-UVSQ, Cedex, France.

<sup>3</sup>LGGE, Laboratoire de Glaciologie et Géophysique de l'Environnement, CNRS, Université Joseph Fourier-Grenoble, Cedex, France.

<sup>4</sup>CECS, Centro de Estudios Científicos, Valdivia, Chile.

<sup>5</sup>Department of Geophysics, University of Copenhagen, Copenhagen, Denmark.

*et al.*, 2006] and ACW (Antarctic Circumpolar Wave with periodicities of 4–5 years and taking 8–10 years to entirely encircle the continent). Modeling studies have suggested a possible atmospheric connection between Antarctic variability and ENSO [Ichiyangi *et al.*, 2002; Werner and Heimann, 2002]. However understanding the influence of such climate modes on local variability (temperature, precipitation, atmospheric circulation) is strongly limited by the availability of reliable and long observations, especially at high altitudes at the border between Northern and Southern Chile.

[3] In this regard, the Patagonian ice fields appear as an excellent candidate to fill that gap. Paleoclimate information is available in Patagonia over time periods varying from a few centuries-tree rings studies in the Argentinian Northern Patagonia revealing that the 20th century contains the longest dry periods over the past 400 years, and that during the same time the mean air temperature increased from about 0.9°C [Villalba *et al.*, 1998 and 2003]- to a few thousand years-data from marine sediment cores extracted from the Chilean continental slope at 41°S allowing us to reconstruct the rainfall variability in relation with the position of westerlies over the past 7700 years [Lamy *et al.*, 2001]. In addition to those climate archives, ice cores provide a unique way to investigate a large set of continuous indicators of both atmosphere dynamic and composition. This is the reason why several firn and ice cores were recovered over the last decades from Northern (NPI) and Southern (SPI) Patagonia icefields.

[4] Six cores have been recovered from the accumulation areas of glaciers in Patagonia. A 14.5-m deep core was drilled at Nef Glacier (1500 m) and a 37.6-m deep core was drilled at San Rafael Glacier (1300 m) on the NPI, but they were found not suitable for paleoclimate reconstructions due to large annual accumulation rates (2.2 m w.eq and 3.5 m w.eq., respectively) and alteration by water percolation [Matsuoka and Naruse, 1999; Yamada, 1987]. A similar problem was encountered near the ice divide at Tyndall Glacier on the SPI where the highest accumulation rate observed in Patagonia was found at an altitude of 1760 m from a 43-m long core [14 m w.eq., Shiraiwa *et al.*, 2002]. At those three sites (Nef, San Rafael and Tyndall) a water-soaked layer was found at the firn/ice interface, which constitutes a water table as it is typically found in the lower accumulation area of temperate glaciers [e.g. Blindow and Thyssen, 1986]. Two shallow cores of 4 and 3 m-depth were retrieved at altitudes of 1540 m and 1840 m at Paso Marconi and Cerro Gorra Blanca Sur respectively (SPI), finding ice in the lower parts of these cores and strong alteration by water percolation [Schwikowski *et al.*, 2006].

[5] Two shallow firn cores have been extracted at higher elevation sites in the SPI accumulation areas: a 13.2-m long core from a point close to the ice divide of Moreno Glacier at an altitude of 2000 m [Aristarain and Delmas, 1993] and a 5-m long core from the plateau of Gorra Blanca Norte at an elevation of 2300 m [Schwikowski *et al.*, 2006]. Average accumulation rates of 1.2 m w.eq. and 1.0 m w.eq. were found at the Moreno and the Gorra Blanca Norte sites respectively. The Moreno core consisted of temperate firn and the chemical species were partly destroyed by water percolation, but the isotopic signals were found to be well preserved. At the Gorra Blanca Norte site, both the chemical

species and the isotopic composition of the ice were found to be well preserved.

[6] On the basis of the conclusions of those previous experiences, we decided to explore the summit plateau of Monte San Valentín (46°35'S, 73°19'W), the highest summit in Patagonia located on the north eastern border of the NPI.

## 1.2. Description of the Site

[7] The field campaign, led by a joint IRD (Institut de Recherche pour le Développement, France) and CECS (Centro de Estudios Científicos, Chile) expedition, was conducted in March 2005 on the summit plateau of Monte San Valentín which has an east–west extension of 1.5 km and spans an altitude range between 3700 m and 4030 m. The drilling site (46°35'19"S, 73°19'39"W, 3747 m) was chosen at the central section of the plateau, within the summit saddle area (Figure 1). The summit of Monte San Valentín is assigned an altitude of 3910 m a.s.l. in the Chilean official maps [JGM, 1982], but a more precise altitude of 4032 ± 1 m a.s.l. is calculated from recent measurements with differential GPS (J. Wendt, personal communication). The drilling site is located in the upper accumulation area of Glaciar San Rafael, ~100 m south of the divide of Glaciar Grosse [Rivera *et al.*, 2007].

[8] No meteorological data are available at the San Valentín summit. We thus use reanalyses and satellite data sets, centered at [46.25°S; 73.75°W], to explore the seasonal variations for (1) temperature, (2) precipitation and (3) wind speed (interannual variations are discussed in section 3.1):

[9] (1) Atmospheric temperatures at 600 mbar (corresponding roughly to an altitude of 4100 m) from NCEP-NCAR (National Centers for Environmental Prediction-National Center for Atmospheric Research Analysis) reanalyses (available at 2.5°) and ERA-40 reanalyses (from the European Centre for Medium-range Weather Forecast, available at ~125 km) [Kalnay *et al.*, 1996; Uppala *et al.*, 2005] are in pretty good agreement at the seasonal timescale over the 1960–2001 period. They show a strong seasonal cycle with lowest (highest) temperatures from June to August (from December to February) of  $-17.2 \pm 0.4^\circ\text{C}$  ( $-10.5 \pm 0.2^\circ\text{C}$ ) and an annual mean surface temperature of  $-13.7 \pm 0.2^\circ\text{C}$ .

[10] (2) For precipitation, the most popular data sets is the Global Precipitation Climatology Project, GPCP, available at 0.5° from 1979 to 2005 [Adler *et al.*, 2003]. Monthly contributions to annual precipitation ( $\sim 3 \text{ mm d}^{-1}$ ) range from 5 (February) to 12.5% (June). However, it is worth noting that over the common period (1979–2001), ERA-40 reanalyses and GPCP data sets are in very good agreement and show almost no seasonality for precipitation (monthly contributions range from 7 to 9.5%) and an annual mean of  $8.8 \text{ mm d}^{-1}$ . This suggests that the 2002–2005 period in GPCP data sets presents very low values all over the year and may alter the average signal.

[11] (3) At last, NCEP-NCAR wind speed reanalyses over the 1948–2005 period indicate that very strong winds prevail in the region of the San Valentín with an annual mean of  $15 \text{ m s}^{-1}$ , and maximum values attaining more than  $20 \text{ m s}^{-1}$  from December to April.

## 1.3. Drilling Operations and On-Site Measurements

[12] A portable solar-powered electromechanical drilling system was used to extract a 15.26-m long and 58-mm

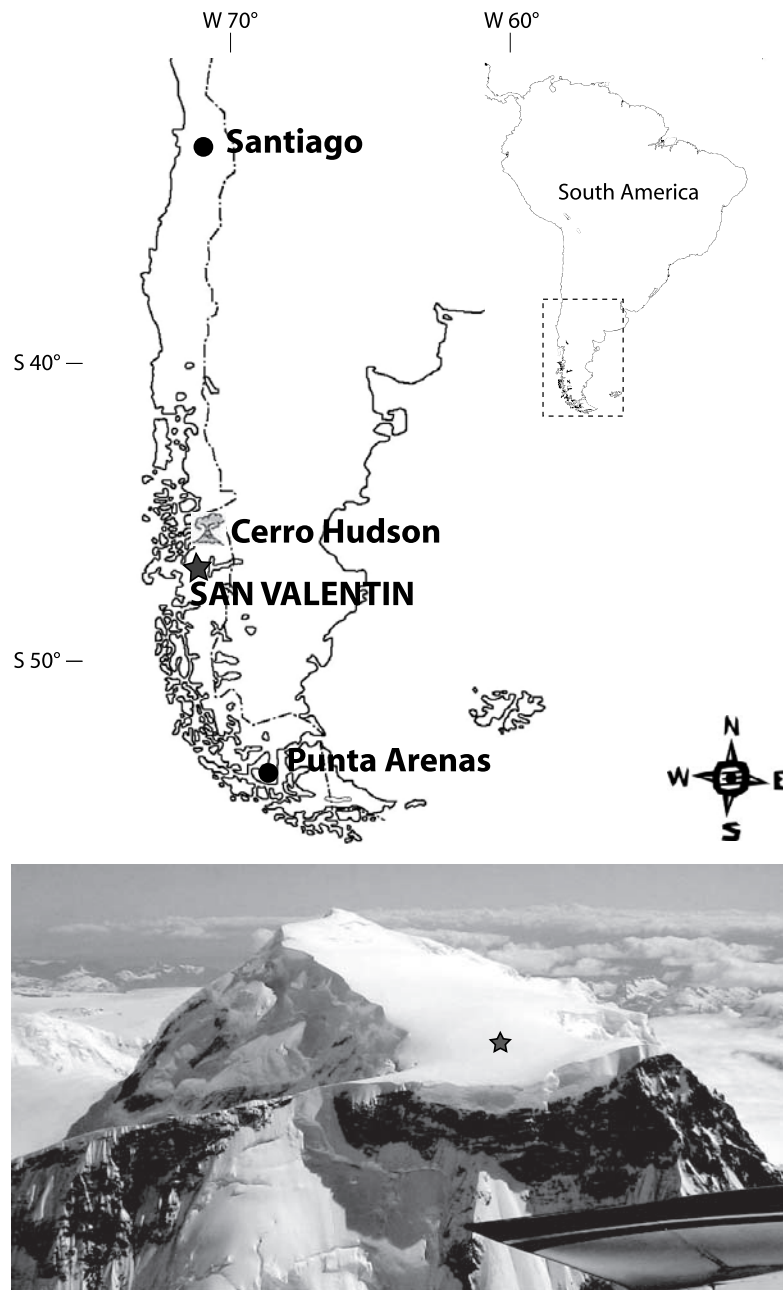


**Figure 1.** Location map and picture of Monte San Valentín in the Northern Patagonia Icefield, Chile. The star shows the position of the drilling site ( $46^{\circ}35'19''\text{S}$ ,  $73^{\circ}19'39''\text{W}$ , 3747 m). Location of Volcán Hudson, 80 km N–NE from Monte San Valentín, is also shown.

diameter firn core [Ginot *et al.*, 2002 and see for example the short video at [http://www.canal.ird.fr/sommaires/missions\\_cp.htm](http://www.canal.ird.fr/sommaires/missions_cp.htm)].

[13] Three radar profiles were measured around the drilling site with a 9 MHz impulse radar system [Casassa and Rivera, 1998] to show that the glacier thickness is 70 m close to the ice divide, increases to 100 m at the drilling site and reaches 170 m on the south-central portion of the summit plateau. Borehole temperature ranges from  $-11.9^{\circ}\text{C}$  at 10 m to  $-11.6^{\circ}\text{C}$  at 16 m depth, allowing to expect well preserved glaciochemical signals. This value is consistent with both the temperature of  $-11.4^{\circ}\text{C}$  calculated for an altitude of 3800 m,

using an altitudinal lapse rate of  $0.5^{\circ}\text{C}/100\text{ m}$  for the NPI [Inoue *et al.*, 1987] and the annual averaged temperature of  $7.7^{\circ}\text{C}$  at Cochrane ( $47^{\circ}15'\text{S}$ ,  $72^{\circ}35'\text{W}$ , 196 m) as a reference value at an altitude of 200 m, and the NCEP-NCAR and ERA-40 reanalyses temperatures at 600 mb given the difference in altitude (see previous section). The core is mostly composed of compact fine grained firn with density increasing from  $0.35\text{ g cm}^{-3}$  at the surface to  $0.6\text{ g cm}^{-3}$  at 15-m depth. Four melting–refreezing ice layers, a few millimeters thick, were observed at 2.20 m, 9.23 m, 9.80 m, and 14.22 m, showing that only very restricted post-depositional modifications by percolation may have occurred.

#### 1.4. Analyses and Methods

[14] The core firn was packed in the field in polyethylene bags and shipped frozen to France.

[15] Continuous concentration profiles were established by ionic chromatography (IC) for inorganic (fluor, chloride, methane sulfonate, nitrate, sulfate, sodium, ammonium, potassium, magnesium, calcium) and mono and di-carboxylic ions (acetate, formate, oxalate, succinate, gluconate) with a resolution of 4–5 cm and typical analytical precision varying from 1% for major ions to ~10% for more sensitive species at low concentration levels (mainly fluoride and carboxylates). Ice sections for IC analysis were cut and subsampled in the LGGE (Laboratoire de Glaciologie et Géophysique de l'Environnement) cold room facilities, using a dry cleaning equipment previously checked and intensively used for Antarctic firn and ice cores. The dry cleaning procedure is based on two steps: cutting ice lamella of 3 per 2.5 to 3 cm thick along the inner part of the core with a band saw, and removing 3 successive layers 1 mm thick along each side of the lamella with a rabot.

[16] The firn isotopic composition (oxygen 18 and deuterium, hereafter  $\delta^{18}\text{O}$  and  $\delta\text{D}$  respectively or  $\delta$ ) has been measured with a resolution of 7–10 cm and an accuracy of  $\pm 0.05\text{‰}$  and  $\pm 0.5\text{‰}$  respectively. The profile resolution is twice lower compared with chemical measurements because we were limited by the possible number of analyses and we expected an important accumulation rate.

[17] Core sections were processed for natural and artificial radioactivity measurements by low-level gamma spectrometry with a continuous sampling every 60–70 cm. Using a method developed by *Delmas and Pourchet* [1977], snow and ice core samples (150–250 g) were melted, weighed, acidified and filtered on ion exchange paper, where all radionuclides were trapped. After drying, the filters were directly analyzed by (1) gamma spectrometry using a very low background specified (type N) coaxial germanium detector (coupled to an anti-Compton device system) of 20.6% relative efficiency and by (2) an alpha/beta low-level radioactivity counting system comprising ten ultra-flat flow  $2\pi$  counter tubes (proportional counter chambers with P10 gas) connected in anti-coincidence with a large-area flow counter tube acting as common guard counter. Measurements were realized at the LGGE semi-buried laboratory, where both analyzers are protected against all interfering ambient radioactivity. (1) The high resolution gamma spectrometry system provides a lower detection threshold, especially for the isotopes of interest such as  $^7\text{Be}$  (54 d),  $^{137}\text{Cs}$  (30.2 years),  $^{210}\text{Pb}$  (22.3 years) and  $^{241}\text{Am}$  (432.7 years), daughter of  $^{241}\text{Pu}$  (14.4 years) with 20, 10, 4 and 2 mBq kg<sup>-1</sup> as detection limit values, respectively. (2) The low-level beta counters exhibit detection levels closed to 20 cph kg<sup>-1</sup> for gross beta counting ( $^{137}\text{Cs}$  and  $^{90}\text{Sr}$ ). Calibrated sources derived from radionuclide liquid solutions (LEA-CERCA or Amersham laboratories) are used to calibrate detectors (methodology and counting efficiency measurements). The analytical procedures were the same as those used for the snow samples. For the present work and because of the low concentrations in the core, accuracies for our measurements are about 20–30% for  $^7\text{Be}$ ,  $^{137}\text{Cs}$  and  $^{241}\text{Am}$ , and more than 50% for  $^{210}\text{Pb}$  in gamma spectrometry, but less than 5% in beta counting. Preliminary data for  $^3\text{H}$  are also available.

[18] The dating of the firn core is detailed in section 2 and major results, in terms of source areas and transport dynamics, are presented and discussed in section 3, demonstrating the suitability of this site for deeper drilling operations and high resolution paleoenvironmental and paleoclimate investigations.

## 2. Firn Core Dating and Snow Accumulation Rate

[19] The dating is made using three independent approaches: the natural radioactive material decay of  $^{210}\text{Pb}$ , the identification of prominent horizons of known ages from radioactive fallout after atmospheric thermonuclear test bombs ( $^{137}\text{Cs}$ ,  $^{90}\text{Sr}$  and  $^{241}\text{Pu}$ , the latter being indirectly measured by  $^{241}\text{Am}$ ) and the counting of continental dust arrival seasonal cycles. This dating is supported by the presence between 5 and 5.3 m of a hudge peak of halite accompanied by a significant peak of HCl which may be attributed to the 1991 Volcán Hudson eruption. We also discuss in this section the lack of seasonal cycles in water stable isotopes. At last, we carefully list some important caveats about this dating.

### 2.1. Radionuclides Species

[20] The natural decay of  $^{210}\text{Pb}$  can be used to estimate the age of firn cores over the recent period (half life is 22.3 years) [*Goldberg*, 1963]. The atmosphere is the major source of  $^{210}\text{Pb}$  deposited on ice sheets and the nuclear explosions in the fifties and sixties have not significantly changed the quantity of deposited  $^{210}\text{Pb}$  [*Bull*, 1971]. Thus provided that we assume a constant annual atmospheric  $^{210}\text{Pb}$  input in the snow and we observe no vertical transportation by water from melting snow [see section 2.4.2. Age estimates in *Eisen et al.*, 2008],  $^{210}\text{Pb}$  profiles along the ice core can be used for dating purposes at any time over the past 100 years. By the application of the Constant Flux Constant Sedimentation  $^{210}\text{Pb}$ -derived model, using the radioactive decay properties [CFCS, *Goldberg*, 1963; *Krishnaswami et al.*, 1971], the  $^{210}\text{Pb}$  specific activity profile at the San Valentín site allows us to estimate an age of  $46 \pm 12$  years at 15.3 m which corresponds to a mean snow accumulation rate of  $33 \pm 9$  cm year<sup>-1</sup> (i.e.,  $17 \pm 5$  g cm<sup>-2</sup> year<sup>-1</sup>) (Figure 2).

[21] Because of (1) the interannual variation of natural  $^{210}\text{Pb}$  annual flux (mainly due to snow precipitation variability), (2) the very low activities detected in our work as observed in most of the high mountain sites (up to 3000 m), and (3) the absence of data knowledge concerning deposition fluxes in our study sector [*Preiss et al.*, 1996], the  $^{210}\text{Pb}$ -based chronology needs to be confirmed by independent methods [*Smith*, 2001] with artificial radionuclide profiles providing unambiguous chronostratigraphic markers. In the Southern Hemisphere, the maximum fallout peaks of fission products ( $^{137}\text{Cs}$ ;  $^{241}\text{Pu}$ , indirectly measured by  $^{241}\text{Am}$ ; and  $^{90}\text{Sr}$ ) are clearly associated with the most intensive testing activity between 1961 to 1962, leading in the southern South America to subsequently fallout with the highest fluxes in 1964 and 1965 [*Arnaud et al.*, 2006; *Magand and Arnaud*, 2007].  $^{241}\text{Am}$  is used to corroborate  $^{137}\text{Cs}$  dates in case of possible disturbance of

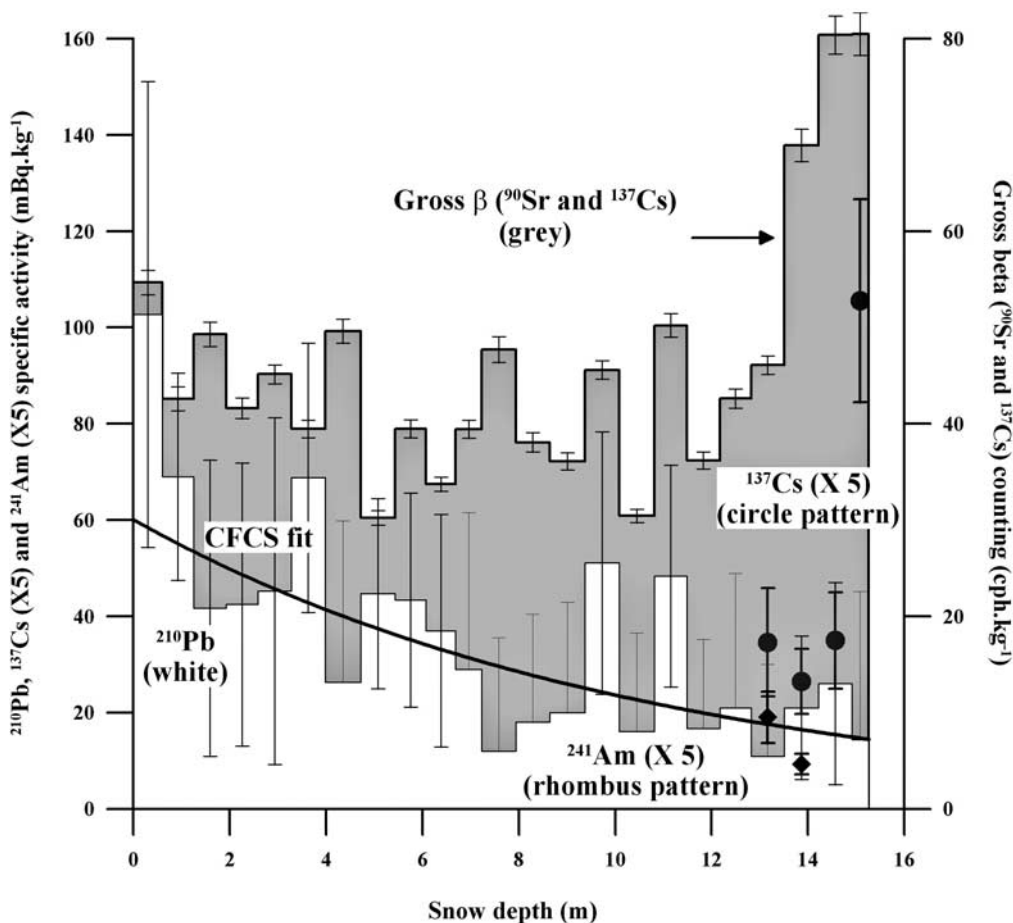


**Figure 2.** Radionuclide profiles (gamma emitters,  $^{137}\text{Cs}$ ,  $^{210}\text{Pb}$ ,  $^{241}\text{Am}$  as well as beta emitters,  $^{90}\text{Sr}$  plus  $^{137}\text{Cs}$ ) used for the San Valentín 2005 shallow firn core dating. The CFCS  $^{210}\text{Pb}$ -derived model fit (bold line,  $n = 23$ ,  $r^2 = 0.5$ ,  $P < 0.05$ ) is also presented.  $^{210}\text{Pb}$  (white area),  $^{137}\text{Cs}$  (gray circle) and  $^{241}\text{Am}$  (black rhomb) are given in specific activities ( $\text{mBq kg}^{-1}$ ) while gross beta activities (grey area) are expressed in counts per hour per kilogram ( $\text{cph. kg}^{-1}$ ). Error bars are expressed as 95% confidence level.  $^{137}\text{Cs}$  and  $^{241}\text{Am}$  scales are multiplied by 5.

the  $^{137}\text{Cs}$  profile [Appleby et al., 1991; Oldfield et al., 1995; Pourchet et al., 2003; Eisen et al., 2008].

[22] Gamma spectrometry profile of  $^{137}\text{Cs}$  (noncorrected from nuclear decay) shows a marked increase in the deepest part of the core (Figure 2), between 13.5 and 15.2 m. No trace of  $^{137}\text{Cs}$  was detected in the San Valentín core between the surface and 13.5 m. A marked increase in the gross beta profile ( $^{137}\text{Cs} + ^{90}\text{Sr}$ ) is also visible at the bottom of the ice core, in agreement with the gamma one. The fingerprint of nuclear weapon tests is also visible in a preliminary  $^3\text{H}$  activity measurement showing a significant value ( $2.34 \pm 0.35$  TU) between 14.7 and 15.2 m depth (one mean sample, U. Schotterer, personal communication). Finally, traces of  $^{241}\text{Am}$  are only detected between 12.8 and 14.2 m depth in the San Valentín firn core. Given the low specific activities and associated high standard deviation of  $^{241}\text{Am}$  analysis, we cannot assume definitively that this last radionuclide does not exist in deeper layers.

[23] The firn core is too shallow to allow us to access to a depth representative of natural gamma and beta radioactive background [i.e., prior to the 1952]. Therefore, we can definitely not attribute radioactivity maximum levels at

the bottom of the core to the fallout products of the northern and southern bomb test periods that peak in 1964–1965. However traces of  $^{241}\text{Am}$ , presence of higher  $^{137}\text{Cs}$  and gross beta activities at the bottom of the core and the rapid decrease of the latter ending between 14.2 and 12.1 m suggest that the 1964–1965 fall out peak is located in the deepest part of the core or slightly before (we remind here that our measurements are made on 70 cm-length ice sections which could represent several years, see also next sections).

[24] Accounting for the above uncertainties, the mean snow accumulation rate deduced from artificial radionuclide fall out can be estimated to  $35 \pm 3$   $\text{cm year}^{-1}$  (i.e.,  $18 \pm 2$   $\text{g cm}^{-2} \text{ year}^{-1}$ ), which is close to the rate obtained from the CFCS  $^{210}\text{Pb}$ -derived model data previously cited. We present in the next section, the independent results from continental inputs seasonal cycles counting.

## 2.2. Calcium Seasonal Cycles Counting

[25] Calcium is a major and very soluble component of erodible soils. It is therefore commonly used as a marker of eolian dust deposits in IC investigations, once the

contribution related to marine primary aerosol input has been removed. Except in very cold marine environment where mirabilite precipitation leads to a bias in sodium content of marine primary aerosol [Wagenbach *et al.*, 1998], the continental  $\text{Ca}^{2+}$  component, denoted  $_{\text{nss}}\text{Ca}^{2+}$  (i.e., nonsea salt calcium), is calculated using sodium concentration as the marine primary aerosol reference and the bulk sea water calcium to sodium ratio, according to  $_{\text{nss}}\text{Ca}^{2+} = \text{Ca}^{2+} - \text{Na}^+ \times (\text{Ca}/\text{Na})_{\text{sea water}}$ .

[26] The nonsea salt contribution of calcium along the San Valentín core is by far the dominant calcium component accounting for  $84 \pm 30\%$  (mean value and standard deviation for the whole core) of total  $\text{Ca}^{2+}$  concentration. The  $_{\text{nss}}\text{Ca}^{2+}$  profile exhibits a rather regular succession of relative maxima and minima superimposed to background large scale variations. An interesting finding is that  $_{\text{nss}}\text{Ca}^{2+}$  mean concentration ( $0.280 \pm 0.005 \mu\text{Eq. l}^{-1}$ ) and peak mean value ( $0.9 \pm 0.6 \mu\text{Eq. l}^{-1}$ ) at San Valentín are rather similar to what was measured with a similar sampling resolution over the past two hundred years in Central Greenland, significantly influenced by continental input after the spring breakdown of the polar vortex [ $0.4 \pm 0.4$  and  $0.8 \pm 0.4 \mu\text{Eq. l}^{-1}$  respectively, *de Angelis and Legrand*, 1995].  $_{\text{nss}}\text{Ca}^{2+}$  mean value is also in the same range as what was measured in rain samples at Torres del Paine, a Southern Chilean Patagonia site surrounded by semi-arid soils [ $_{\text{nss}}\text{Ca}^{2+}_{\text{annual mean}} = 0.5 \mu\text{Eq. l}^{-1}$ , *Galloway et al.*, 1996]. Such similarities lead us to conclude that significant amount of aeolian dust regularly reaches the San Valentín summit area, which could seem puzzling considering the prevailing wind direction from west sector over southernmost South America. However the existence of large dust sources in South America combined to the occasional occurrence of favorable regional or meso-scale meteorological patterns make such influence quite possible allowing to interpret  $_{\text{nss}}\text{Ca}^{2+}$  depth-variations in terms of seasonal trends. Indeed: (1) they are three persistent dust sources in South America: the first one is located, farther north, in the Bolivian Altiplano ( $19\text{--}20^\circ\text{S}$ ,  $67\text{--}68^\circ\text{W}$ ), and the two others are located in central Patagonia (Argentina), roughly encompassed by [ $37\text{--}45^\circ\text{S}$ ,  $66\text{--}70^\circ\text{W}$ ] and by [ $27\text{--}34^\circ\text{S}$ ,  $67\text{--}70^\circ\text{W}$ ]. Preferential dust mobilization is observed from September to February [*Prospero et al.*, 2002], when the cloud cover vanishes and aridity increases [*Paruelo et al.*, 1998; *Diaz et al.*, 2006]; (2) although the main wind direction at  $45^\circ\text{S}$  is westward over Patagonia, calm events occur mostly in winter but also in summer, a southerly component is evident in summer [*Paruelo et al.*, 1998], and occasional strong wind events from Eastern sector occur throughout the year over semi-arid areas of central east Patagonia [ $\sim 11\%$  of major wind events, *Labraga*, 1994]; (3) Meridional transport of black carbon from tropical burning areas in Brazil to the northern Antarctic Peninsula has also been evidenced and related to intermittent mechanism involving the low-level jets east of Andes, the displacement eastward of frontal systems passing over Drake Passage and the high pressure over the Atlantic Ocean associated with the subtropical height [*Pereira et al.*, 2006]. Andean summital areas are on the boarder of such southward flow. Taken together, all these considerations support the regular occurrence of aeolian

dust flux likely mostly from eastern central patagonian areas at the top of San Valentín.

[27] Considering precipitation and wind annual mean patterns over source areas, such input is expected to be maximum in austral spring-summer. Assuming that  $_{\text{nss}}\text{Ca}^{2+}$  high frequency oscillations are related to seasonal changes in aerosol production and transport with maximum occurring from September to February, we have considered that every firn layer containing one relative maximum surrounded by two relative minima correspond to one annual layer,  $_{\text{nss}}\text{Ca}^{2+}$  spring-summer maxima being taken as markers of the beginning of every civil year. According to this assumption, thirty-nine annual layers denoted by vertical arrows in Figure 3 are evidenced along the core, leading to a date of 1965 at the bottom of the core and a mean snow accumulation rate of  $39.1 \text{ cm year}^{-1}$  ( $20.4 \text{ g cm}^{-2} \text{ year}^{-1}$ ), which fits pretty well the time range deduced from radio-nuclides data. Interestingly,  $_{\text{nss}}\text{Ca}^{2+}$  peaks are rather large (2–3 samples, i.e., 10–15 cm) which strongly suggests that they correspond to dust deposited during precipitation events. Question marks in Figure 3 show a few possible other annual layers that are more debatable, because they correspond to  $_{\text{nss}}\text{Ca}^{2+}$  peaks restricted to one sample which may thus be related to seldom sublimation events occurring within a year. Regardless, taking into account those peaks denoted by question marks would lead to date the bottom of the core in 1961 and to decrease the mean accumulation rate by  $3.6 \text{ cm year}^{-1}$  ( $1.9 \text{ g cm}^{-2} \text{ year}^{-1}$ ).

### 2.3. A Possible Additional Time Marker: The 1991 Volcán Hudson Eruption

[28] Volcán Hudson (1905 m), located 80 km N–NE from Monte San Valentín (Figure 1), erupted most recently in two separate cycles on August 8th and August 12th, 1991. The August 8–9 eruption produced a dense ash column 7 to 10 km high which subsequently rose to 12 km. Both the ash and aerosol plumes were transported in a N–NE direction and ash was deposited with an elliptical isopach distribution (N–NE axis) over southern Chile [*Moxey*, 2004]. In the second most powerful eruption of 12–15 August, the volcanic plume was transported SE–E [*Moxey*, 2004] with a maximum column height of 17 km [*Naranjo et al.*, 1993]. Large volumes of ash were deposited according to an elliptical isopach direction (SE) over Chile and Argentina. Ashfall was observed on the Falkland islands ( $\sim 1000 \text{ km SE}$ ) and reached Antarctica [*Smellie*, 1999]. Satellite data showed that the eruption produced a large  $\text{SO}_2$ -rich cloud, estimated to contain 1.5 megatons of  $\text{SO}_2$  on 16th of August. Most of the sulfur species (early volcanic  $\text{H}_2\text{S}$  and  $\text{SO}_2$ ) were injected at high altitude and transported twice around the globe in 2 weeks. They were oxidized as  $\text{H}_2\text{SO}_4$  in roughly one month [*Rose et al.*, 2000]. The question we now ask is: is there a signature of the 1991 Cerro Hudson eruption in the San Valentín record? To answer this question, several chemical indicators presented and discussed in greater detail in section 3 are used. Although the main volcanic cloud of Volcán Hudson moved southeast, passing about 30 km east of San Valentín, some fingerprints may be expected along the firn record, more likely as dust layer (soluble and insoluble) or gas having diffused from the lower part of the plume or scavenged by water condensation. Because of the very small diameter of our preliminary core, insoluble dust content was

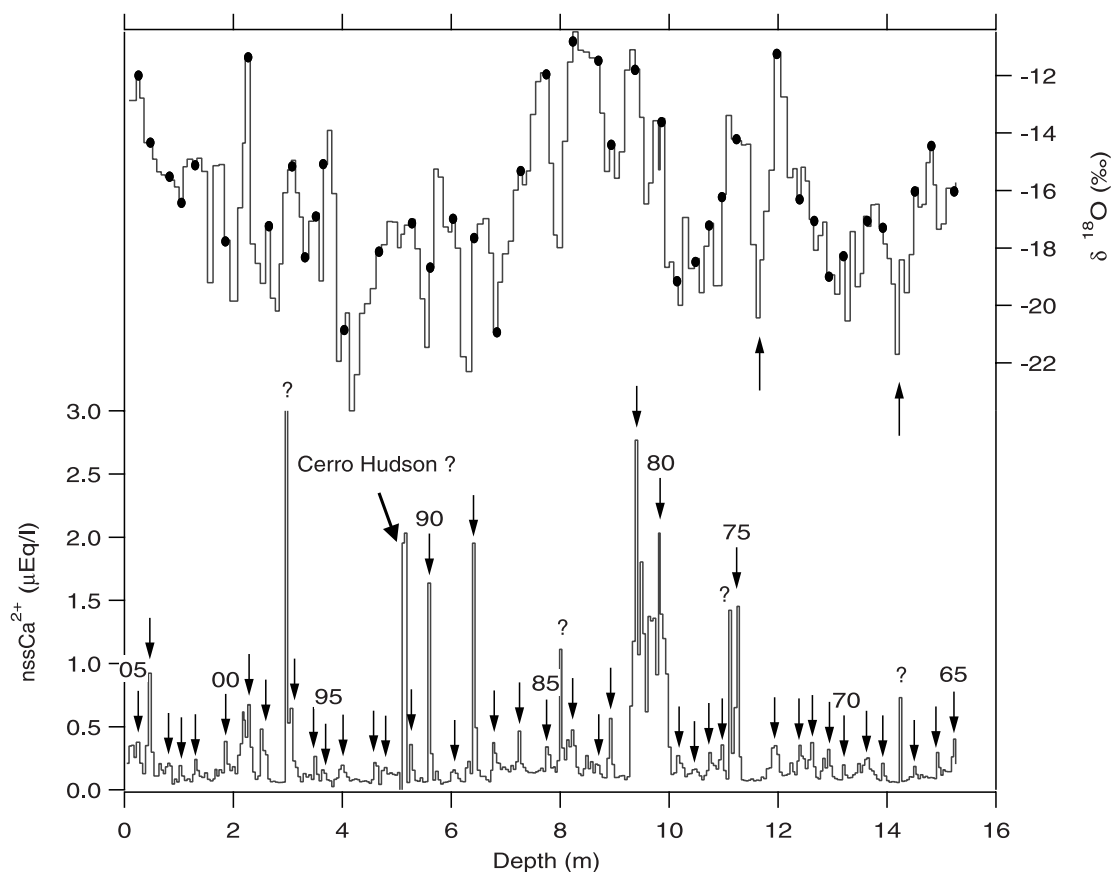


**Figure 3.**  $\text{nssCa}^{2+}$  ( $\mu\text{Eq l}^{-1}$ ) used for the annual layers counting and  $\delta^{18}\text{O}$  of the ice (‰). On the  $\text{nssCa}^{2+}$  profile, the arrows indicate the different annual layers and the question marks show alternative possibilities for the annual layer counting. On the  $\delta^{18}\text{O}$  profile, we report the age estimated with  $\text{nssCa}^{2+}$  with black dots and the two black arrows show two identified seasonal cycles.

not measured, and the discussion will be only based on soluble species (part of them can be produced during volcanic event).

[29] A huge peak of NaCl, by far the highest of the whole profile and firstly presumed to be of marine origin, was observed at 4.6–5.4 m in the layer dated in 1991 (event A). This event was carefully compared with another large marine event (event B) at 7–8 m, depicted by high Na and Cl concentrations with a ratio close to the marine one. The detailed comparison of indicators of marine primary aerosol ( $\text{Na}^+$ ), marine biogenic production ( $\text{nssSO}_4^{2-}$ , calculated in the same way as  $\text{nssCa}^{2+}$ , i.e., according to:  $\text{nssSO}_4^{2-} = \text{SO}_4^{2-} - \text{Na}^+ \times (\text{SO}_4/\text{Na})_{\text{sea water}}$ , and MSA) and erodible soils ( $\text{nssCa}^{2+}$ ) for these two events is presented in Figure 4 (left: event A, right: event B). We have also reported  $\text{Cl}_{\text{exc}}^-$  which represents the Cl part that is not explained by marine salt ( $\text{Cl}_{\text{exc}}^- = \text{Cl}^- - \text{Na}^+ \times (\text{Cl}/\text{Na})_{\text{sea water}}$ ) and should remain close to zero in marine rich air masses rapidly advected to the drilling site from surrounding ocean. In event B, high sodium concentrations are associated with biogenic sulfur traced by large amounts of MSA and  $\text{nssSO}_4^{2-}$  amounting for about 30% of total sulfate. The  $\text{Cl}^-$  to  $\text{Na}^+$  ratio remains very close to the bulk sea water value during the whole event, corresponding to a very low and slightly negative  $\text{Cl}_{\text{exc}}^-$  value (mean value of  $0.6 \mu\text{Eq l}^{-1}$ , standard deviation of  $0.2 \mu\text{Eq l}^{-1}$ ). This fits what is expected for marine aerosol (see the discussion on

marine primary aerosol in section 3.3). Event A appears quite different: while  $\text{Na}^+$  concentrations are more than 5 times higher than during event B, MSA remains in the background range and  $\text{nssSO}_4^{2-}$  is negative. At the same time, a large continental dust contribution shown by  $\text{nssCa}^{2+}$  and a peak of HCl ( $\text{Cl}_{\text{exc}}^- \text{ max} = 6.4 \pm 2.4 \mu\text{Eq l}^{-1}$ , rather high analytical uncertainty being related to the very large amounts of chloride and sodium) are observed. It is worth noting that there are only two peaks of HCl along the whole profile—peak in event A and a smaller one dated in 1975 and attributed to a large fire event (see section 3.2 for details)—and that we do not observe elsewhere in the profile significant  $\text{nssCa}^{2+}$  concentrations associated with large marine aerosol concentrations. Moreover this is the only part of the core where negative  $\text{nssSO}_4^{2-}$  values are observed. Such negative values may be explained by two very different reasons: (1) marine aerosol deposited were sulfate depleted with respect to sea water composition; this is observed in Antarctica during winter when mirabilite precipitates at temperature lower than  $-8^\circ\text{C}$  [see for instance *Wagenbach et al.*, 1998] but cannot be expected at warmer San Valentin latitude and (2)  $\text{Na}^+$  concentrations taken as reference values have a significant continental component leading to overestimate the sea salt sulfate contribution which may become greater than the total sulfate concentration. The large  $\text{nssCa}^{2+}$  peak at this depth and the following discussion led us to propose the

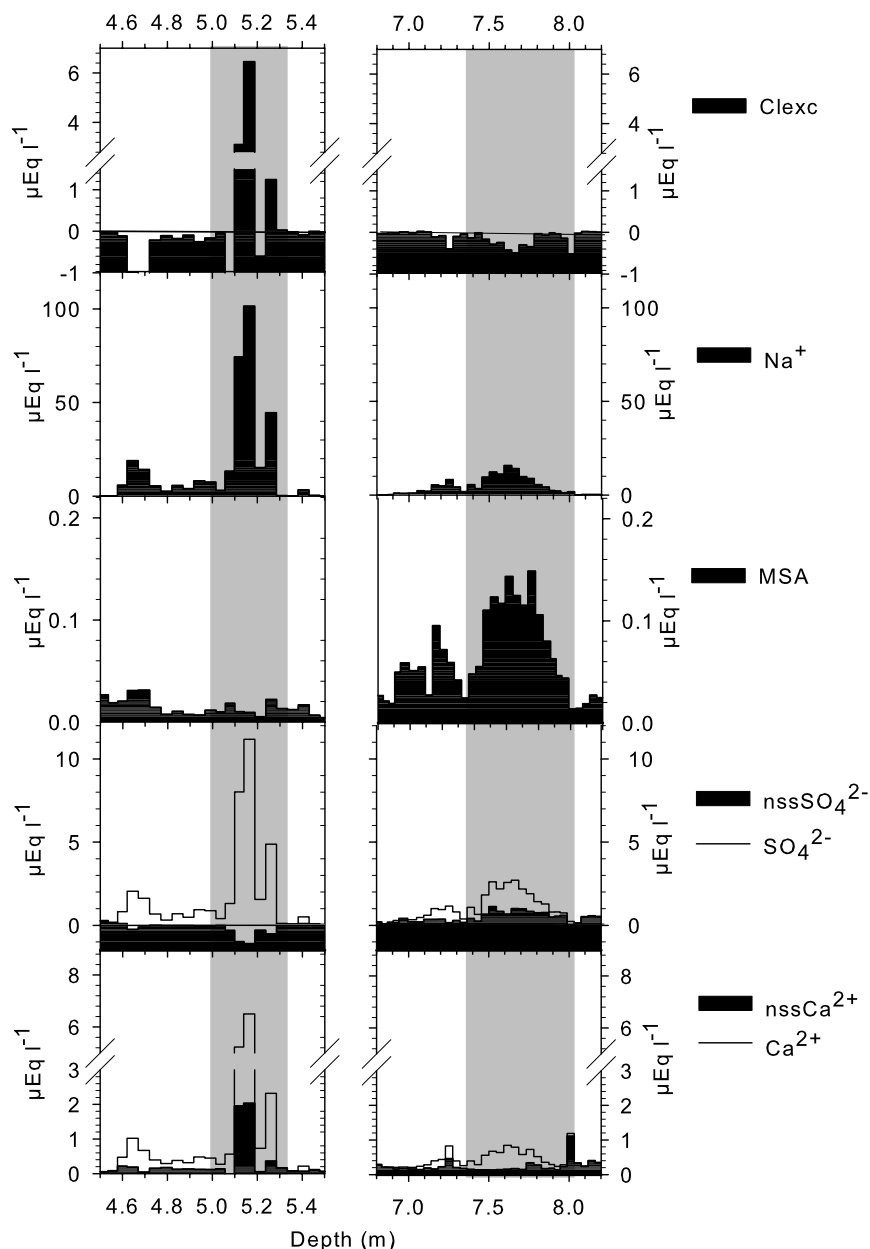


**Figure 4.** Chemical concentration profiles for two different sections of the shallow core. Event A ranges from 4.4 to 5.6 m and event B ranges from 6.8 to 8.2 m.

second explanation for these slightly negative  $\text{nssSO}_4^{2-}$  values. The large differences observed between the salient features of event A and B lead us to consider that the NaCl peak in event A has no marine origin but corresponds to halite mixed with HCl, both species having the same origin possibly volcanic.

[30] Indeed, although the reactions occurring between gases/aerosols and silicate ash particles in volcanic plumes remain poorly understood, it has been observed that halogens (HF and HCl), alter ashes, producing significant amounts of halide salts at the surface of ashes, in particular halite (NaCl) [Stoiber and Rose, 1974; Woods *et al.*, 1985]. As a general rule, halite is one of the predominant species released on the first exposure of volcanic ash to water [Delmelle *et al.*, 2007; Witham *et al.*, 2005]. Because of

the condensation of magmatic water vapor when thermal equilibrium is reached, most of halite is likely scavenged along with other very soluble species before the plume reaches the upper troposphere. Significant halite deposits are thus expected around eruption areas, independently of winds prevailing at higher altitude and carrying away aerosol plumes with ashes and sulfur species. On the contrary, on the basis of the lifetime and the injection height of reduced sulfur species, significant regional deposits of sulfate are not expected windward of the eruption site.

[31] We thus conclude that the 5 m NaCl peak may effectively be related to the early deposits of a rather close volcanic event. That could correspond to the tremendous Volcán Hudson, 1991 eruptions. If so, the reliability of the dating would be reinforced.

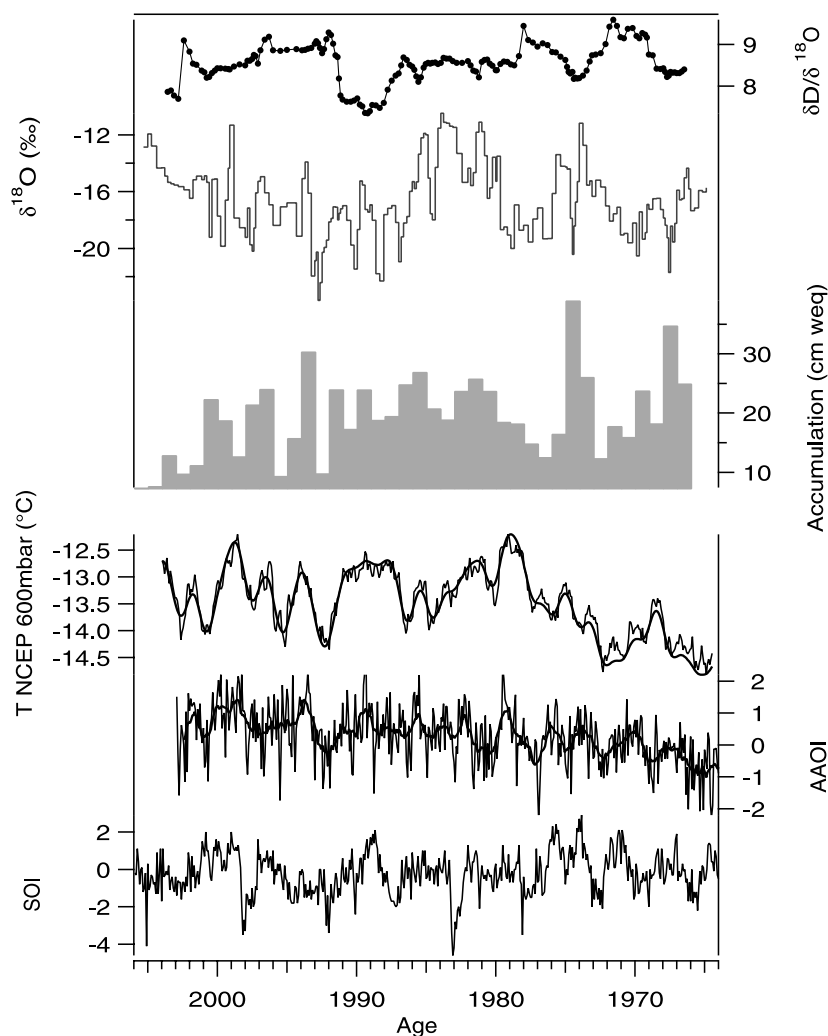


**Figure 5.** From top to bottom:  $\delta D/\delta^{18}O$  running slope over 13 points;  $\delta^{18}O$  of the ice (‰); Accumulation estimated from  $Ca^{2+}_{nss}$  dating (cm weq.); NCEP-NCAR atmospheric temperatures ( $^{\circ}C$ ) at 600 mbar (centering on  $46.25^{\circ}S$ ;  $73.75^{\circ}W$ ) with a 12-point running average (thin line) and first and second principal component obtained from a MTM-SSA analysis (thick line); Antarctic Annular Oscillation Index (AAOI) with a 12-month running average (thick line) and Southern Oscillation Index (SOI).

#### 2.4. The Lack of Water Stable Isotopes Seasonal Cycles

[32] The  $\delta D/\delta^{18}O$  slope is of  $8.64 \pm 0.07$  and the intercept of  $20.5 \pm 1.2$  ‰ ( $r^2 = 0.99$ ,  $n = 177$ ). To examine whether some evaporative processes, such as snow melting, occur at the surface and modify the isotopic composition of snow, a running  $\delta D/\delta^{18}O$  slope is calculated (Figure 5). Actually, meteoric  $\delta D/\delta^{18}O$  slope decreases to around 4.5 when evaporative processes occur. To discuss only significant slopes at 99.9 % (i.e.,  $p = 0.001$ ), we need to calculate slope with at least  $n = 13$  ( $r^2 > 0.64$ ) covering a firn length between 98 cm and 1.26 m. Slopes vary between 7.3 and 9.6 (with an error bar always lower than  $\pm 1.0$ ) confirming no trace of surface melting recorded in the firn core. Calculations of deuterium excess ( $d = \delta D - 8 \times \delta^{18}O$ , discussed in section 3.3) along the firn core confirms the absence of (1) evaporative processes at the snow surface with values varying from 7.7 and 15.3 ‰ in the first 2 m ( $d$  is supposed to be close to zero and even negative in

such cases) and (2) condensation of water vapor in the firn (no specific high values are found in the 4 melt–refreeze layers mentioned in section 2).

[33] It is now well known that at both low and high latitudes, the isotopic composition of precipitation exhibits a clear seasonal cycle because of strong precipitation and temperature seasonal cycles respectively. At mid-latitudes, data collected at stations from the global IAEA network (International Atomic Energy Agency), both in the Northern and Southern hemispheres, clearly show a linear  $\delta/T$  relationship at both seasonal and interannual timescales [Fricke and O’Neil, 1999]. This positive correlation is also clearly shown in atmospheric general circulation models including water stable isotopes [Hoffmann et al., 1998]. Indeed, the isotopic composition of precipitation primarily records the rainout history of airmasses which is intimately related to the condensation temperature variations [Dansgaard, 1964]. The IAEA network is relatively poor in South

America and no IAEA data are available at high altitude in the San Valentín area. At the closest IAEA station, Coyhaique site (45°35'S; 75°07'W, 310 m) located at around 100 km northwest from San Valentín, the monthly isotopic composition of precipitation is available from October 1988 to December 1999. Although a 10-year period is not long enough to significantly discuss the long-term annual  $\delta/T$  correlation ( $n = 10$ ), we can use the long-term monthly data (i.e., the 117 months for which isotopic data exist). For the mean seasonal cycle, the  $\delta^{18}\text{O}/T$  covariation is  $r^2 = 0.82$  ( $n = 12$ ) with a slope of  $0.43\text{‰}/^\circ\text{C}$ , as expected for low elevation sites at mid-latitudes [Hoffmann et al., 1998; Fricke and O'Neil, 1999] (note that the linear fit on all the monthly data leads to a similar slope with  $r^2 = 0.38$  and  $n = 117$ ). Actually, in the Northern Hemisphere, the numerous stations located between 40° and 60°N exhibit together a slope of about  $0.3\text{‰}/^\circ\text{C}$  [Rosanski et al., 1993]. As opposed to Andean tropical areas where around 80% of precipitation is convective, the major part of the west Patagonian precipitation originates from stratiform clouds that develop along warm and cold westerly fronts [Garreaud et al., 2008] and thus the  $\delta/T$  relationship remains valid. It is worth noting that the seasonal  $\delta^{18}\text{O}/P$  covariance at Coyhaique is of  $r^2 = 0.52$  ( $n = 12$ ) with a slope of  $-0.0032\text{‰}$  for every mm/year but it decreases to  $r^2 = 0.11$  when considering all the monthly data ( $n = 117$ , slope of  $-0.0016\text{‰}$  for every mm/year), suggesting only a weak precipitation control on isotopes at monthly scale. Further investigations based on both Atmospheric General Climate Model (AGCM) including water stable isotopes and direct observations will have to be explored to reliably interpret the isotopic composition of San Valentín firn and we cannot exclude any control of precipitation on isotopes at the interannual timescale.

[34] Thus we expected to find some seasonal cycles in the isotopic composition of the San Valentín ice related to seasonal temperature variations ( $\Delta T \sim 7^\circ\text{C}$ , see section 1.2). However we cannot clearly distinguish seasonal variations in agreement with chemical seasonal cycles. Although we seek to associate the seasonal cycles recorded in the  $\text{Ca}^{2+}$  profile to the  $\delta$  record high frequency (black dots in Figure 3), no robust relationship can be pointed out whatever the depth is. Our favorite hypothesis to explain the lack of clear seasonal cycles is the low sampling resolution (7–10 cm). Actually, the number of isotopic measurements between two  $\text{Ca}^{2+}$  peaks is always lower than 6 (most of the time there are 2 (22.5%), 3 (30%) or 5 (25%) measurements) except for 2 years where 7 measurements have been done. In those two cases (between 11.245 and 11.930 m and 13.855 and 14.490 m), we clearly see a seasonal variation in  $\delta$  with the lowest value corresponding to the minima of  $\text{Ca}^{2+}$  which is supposed to occur between June and August, the coldest season (see black arrows on  $\delta$  in Figure 3 and for example the  $\delta^{18}\text{O}$  variation of 10‰ in 1975). Another explanation could be a change in precipitation and/or wind erosion seasonality. A significant change in precipitation seasonality is not recorded in reanalyses over the last 40 years (see section 1.2). However, because of wind erosion, part of the annual snow layer could be missing for specific years, removing any traces of seasonal cycle. It is worth noting that this assumption is not supported by calcium measurements. As explained in section 2.5, snow

layers containing calcium (austral summer) are not significantly eroded by the wind from year to year.

[35] Regardless, it is worth noting that a residual signal of seasonal cycles clearly remains all over the record as it is strongly suggested by an harmonic MTM analysis pointing out a significant signal in the 1- to 2-year band (harmonic peaks are detected by the F-Test between 1.2 and 2.5 years at the 90% confidence level, Mann and Lees [1996], not shown). At the interannual timescale,  $\delta^{18}\text{O}$  exhibits an interesting signal ranging from  $-23.67$  to  $-10.48\text{‰}$  ( $m = -16.61\text{‰}$  and  $\sigma = 2.61$ ) with a strong low frequency of about 9.5 years (85% confidence level) that will be discussed in section 3.1.

[36] At last, we would like to mention that according to our knowledge on other sites, the isotopic diffusion cannot be a possible cause to explain the lack of  $\delta$  seasonal cycles. Actually, on Greenland sites, where mean surface temperatures are lower than at San Valentín, the diffusion length is about 10 cm [Johnsen and Robin, 1983] i.e., 3 times higher than our estimated accumulation.

[37] In conclusion, the low sampling resolution and the wind erosion could explain the lack of seasonal cycles. We discuss in the next section the possible effects of wind erosion from calcium and sodium measurements, done with a higher resolution. Regardless, the lack of  $\delta$  cycles is a handicap to accurately date the shallow core.

## 2.5. Snow Accumulation Rate and Wind Effects

[38] Precipitation at the NPI latitude ( $\sim 46^\circ\text{S}$  to  $47.5^\circ\text{S}$ ) are strongly controlled by orography and the Andean Cordillera is an efficient topographic barrier leading to a decrease of annual precipitation rate from approximately 7000 mm on the Chilean coast (windward) to less than 200 mm east (leeward) of the Argentinean Andes [Carrasco et al., 2002; Schneider et al., 2003; Villalba et al., 2003]. Data previously published for NPI and SPI reveal accumulation rates of several meters of snow per year [Matsuoka and Naruse, 1999; Popovnin et al., 1999; Shiraiwa et al., 2002; Yamada, 1987]. Net snow accumulation rates are lower at the highest drilling sites on SPI, that are Moreno (2000 m, 1.2 m w.eq.) [Aristarain and Delmas, 1993] and Gorra Blanca Norte (2300 m, 1 m w.eq. calculated only on a 5-m long firn core) [Schwikowski et al., 2006]. Compared to these values, the net accumulation rate at San Valentín seems rather low, but not unreasonable taking into account the altitude of the site, which is located 1000–2000 m higher than the other drilling sites.

[39] Nonetheless, the effects of wind erosion should be taken into account when discussing the net accumulation values. Indeed, westerly winds prevailing in Patagonia are intense [Pruel et al., 1998] and NCEP-NCAR reanalyses show that San Valentín is exposed to west winds varying from 17 to more than  $20 \text{ m s}^{-1}$  from December to April. Thus it makes sense to ask the following questions: are there any missing years in the San Valentín record? What is the meaning of the net accumulation that we can calculate for each year?

[40] A detailed examination of chemical profiles provides useful information on the remaining archive. We compare in Figure 6, sodium concentration, taken as a marker of marine primary aerosol and thus related to precipitation associated to west winds, with  $\text{Ca}^{2+}$  concentration, taken as a marker

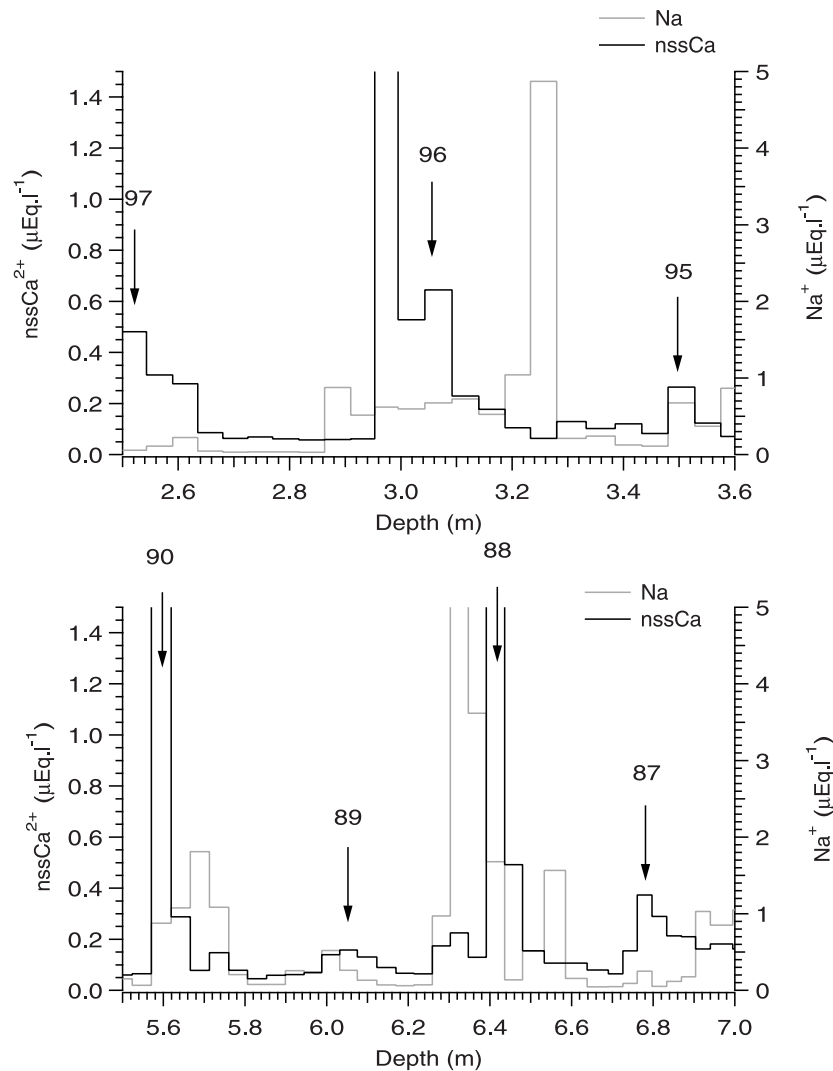


**Figure 6.**  $\text{nssCa}^{2+}$  (black) and  $\text{Na}^+$  (grey) concentrations ( $\mu\text{Eq. l}^{-1}$ ) for two different sections of the firn cores and covering several years.

of E–NE continental arrivals, along two core sections covering approximately 3 years each, based on calcium dating (2.5–3.6 m and 5.5–7 m). Annual maximum of both species is visible and even if rather thin, they are clearly recorded in distinct layers within a year. Despite very different concentration ranges and scattering, this difference in the location of relative  $\text{Na}^+$  and  $\text{nssCa}^{2+}$  maxima may be observed almost every year along the whole profile, which indicates that part of the precipitation from west is also archived every year. On the basis of this calcium and sodium seasonal variability and on the presence of other continental markers along the core (see section 3.2), we can state that no complete year is missing and that the continental fingerprint is rather well documented. This result is not quite surprising. Indeed,  $\text{nssCa}^{2+}$  deposition is likely associated to E–NE precipitation that are less abundant (see section 2.2) and occurring when west winds circulation flags. Thus the snow layers containing calcium should not be significantly eroded by wind. Moreover, during those periods of lower wind, the snow metamorphism should

rapidly lead to the formation of more dense firn, preventing from further erosion.

[41] We calculate the net accumulation arising from  $\text{nssCa}^{2+}$  record for each year considering that a  $\text{nssCa}^{2+}$  peak corresponds to the start of a civil year (Figure 5). Interestingly, the net accumulation does not vary too much ( $19 \pm 7$  cm w.eq.). As  $\text{nssCa}^{2+}$  deposition is rather linked with E–NE precipitation (see above), this net accumulation should correspond to the annual deposit of most of snow not associated to westerlies and thus rather well preserved and to the remaining part of snow associated to westerlies and partly blown off. As an immediate consequence, we thus think there is no sense to regard our net accumulation calculation as a proxy of on site precipitation. Another important consequence is that flux calculation will certainly not be valid for the marine component. Nevertheless, and according to what is observed in clean remote areas with moderate precipitation rate [*de Angelis et al.*, 1997], concentrations of chemical species deposited through wet deposition processes are directly related to atmospheric concentration and thus, even if part of the

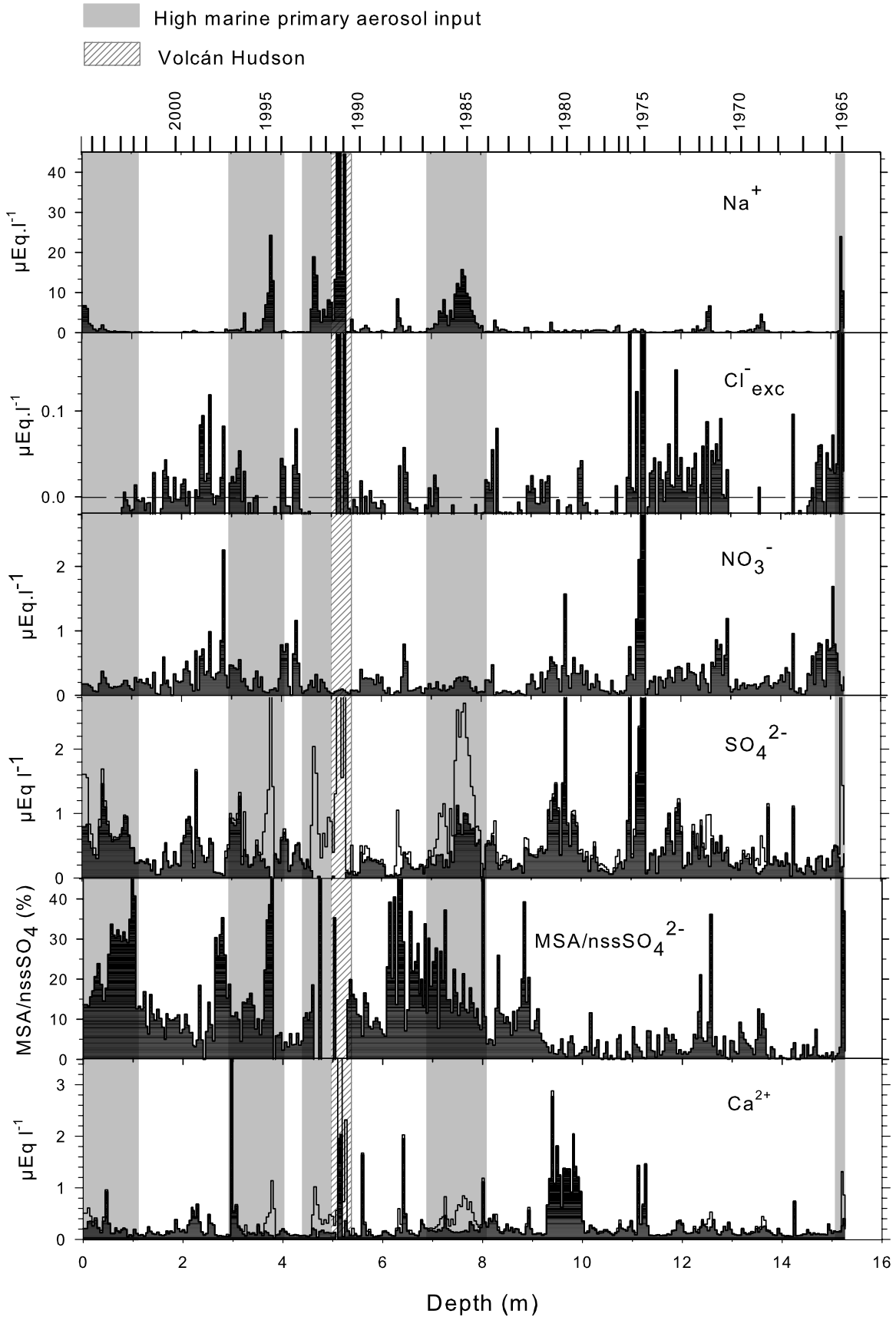


Figure 7

snow is removed, the remaining part should keep reliable information on past atmospheric composition. We further discuss the  ${}_{\text{nss}}\text{Ca}^{2+}$  flux in the section 3.2.1.

## 2.6. Important Caveats and Discussion on the Firn Core Dating

[42] Our different approaches are consistent and focus on a date of 1965 at the bottom of the firn core (15.3 m), leading to an average accumulation rate of  $36 \pm 3 \text{ cm year}^{-1}$  (the standard deviation is estimated by a Monte Carlo sampling of the three distributions with 2000 trials). Although we present here what we think to be an optimal dating based on a rigorous analysis, we would like to mention some important caveats:

[43] (1) It is important to mention that because the rate of both natural and artificial radionuclide fallout is very low in South America [Ribeiro Guevara et al., 2003; Arnaud et al., 2006], radionuclide-derived geochronology at the San Valentín site has not to be overinterpreted. Moreover, present radionuclide profiles prevent us from clearly locating the fallout peak products of major bomb test periods which peaked in 1964–1965 in Southern Hemisphere. This may be due to the low sampling resolution (i.e., 60–70 cm ice section), but with no more precision, the date of 1965 is the oldest we can attribute to the deepest part of the firn core.

[44] (2) It is worth noting that 41 atmospheric French nuclear tests were performed from 1966 to 1974, in French Polynesia (22°S, 158°W). Only a few of them (less than 10%) were in the Megaton range, and most (50%) were less than 20 kt. The Kiloton range nuclear explosions did not penetrate appreciably into the stratosphere [Eisenbud and Gesell, 1997] and under the conditions that normally prevail at the test site, radioactive debris of the local and tropospheric fallout was carried to the east over uninhabited regions of the Pacific (some hundreds km from test site). On rare occasion, some material was transferred to the central South Pacific within a few days of the tests by westerly moving eddies. Only the fission radioactive debris from Megaton range Test series, partly partitioned in stratosphere, were detected in few atmospheric monitoring stations in South America [Magand and Arnaud, 2007]. The total yield production by French nuclear tests was lower than 18 Mt, i.e., less than 105 PBq of rejected  ${}^{137}\text{Cs}$ , compared to approximately 525 PBq of  ${}^{137}\text{Cs}$  produced (and world-wide distributed) during the two-years long most intensive period of tests (1961–62, a period when more than 57% of the total detonation power from 1945 to 1980 was detonated). Then, even if French nuclear tests were detected in some atmospheric monitoring stations in South Hemisphere, the most intense fallout peaks observed in these sampling stations for long-lived fission products ( ${}^{90}\text{Sr}$ ,  ${}^{137}\text{Cs}$ ) were not associated with South Pacific Nuclear tests but with the most intensive period of tests between 1961 and 1962. Although no unambiguous marker allows us to distinguish debris produced by Russian thermonuclear explosions and/or French Pacific nuclear tests, considering the dating inferred from

the  ${}_{\text{nss}}\text{Ca}^{2+}$  profile, the observed decreases of  ${}^{137}\text{Cs}$  and gross beta activities from 14.2 to 12.1 m in the deepest part of the core could be interpreted as the fission products depletion of polar stratosphere following the 1964–1965 maximum fallout peak followed by the possible remaining influence of few French nuclear tests (1966–1974) (Magand and Arnaud, 2007).

[45] (3)  ${}^7\text{Be}$  (half-life of 53 d) has been also measured and is detected down to 2.59 m with a puzzling maximum between 1.26 and 2.59 m. That could suggest an age of about 18 months for this firn ice section. The interpretation of  ${}^7\text{Be}$  in San Valentín snow is difficult because we do not know (1) the initial  ${}^7\text{Be}$  activity (i.e., local  ${}^7\text{Be}$  deposition flux in the study area) in falling snow, (2) the origin of  ${}^7\text{Be}$  measured in the firn core (which could be stratospheric as nitrate also shows high concentration between 1.26 and 2.59 m, see Figure 7), and (3) the relative importance of accumulation and erosion, the latter being involved in snow redistribution after deposition and possibly combining fresh and old snow. However we may have counted too many years at the surface (5 years are counted between 0 and 2 m) as it could be also suggested by the isotopic composition of the ice showing a rather regular increase over the first 1.5 m.

[46] (4) Ash deposits corresponding to volcanic events of moderate importance but potentially useful for dating improvement (like the Volcán Arenales, 47.20°S, 73.48°W, 3437 m located on the NPI and erupted in 1979) may be expected along the core. However, as stated above, the small amount of material available made it impossible to perform the additional analyses required to unambiguously identify volcanic material like glass shards or tephtras in specific layers.

[47] In conclusion, we estimate that our dating has an uncertainty from 1 to 5 years that has to be taken into account when discussing the data.

## 3. Discussion

[48] Chemical species discussed here have been chosen according to their ability to trace past atmospheric circulation and source productivity. Similarly, we discuss here the firn isotopic composition as a possible proxy of atmospheric temperature and deuterium excess as a possible tracer of the origin of air masses.

### 3.1. Which Climate Signal is Recorded in $\delta$ ?

[49] Because no long-term temperature observations are available at San Valentín, we compare the isotopic composition of the ice with the NCEP-NCAR atmospheric temperature reanalyses at 600 mb, centered at [46.25°S; 73.75°W], and available until June 2004 (corresponding roughly to the atmospheric surface temperature at the San Valentín site, see section 1.2). The monthly temperature at 700 mb from 1965 to 2004 exhibits very similar intra- and interannual variations, shifting only the signal by about

**Figure 7.** Selected chemical concentration profiles ( $\mu\text{Eq. l}^{-1}$ ). Calcium total concentrations are denoted by the black line, nonsea-salt calcium corresponds to the curve with black back-plane, same for sulfate. The parts of profiles superimposed to gray areas (different from Figure 4) correspond to periods of high marine aerosol inputs and the area overlined by dashed bars indicates the possible Volcán Hudson location.

+6°C ( $T_{700\text{mb}} = 0.92 T_{600\text{mb}} + 5.7$ ,  $r^2 = 0.99$ ,  $n = 485$ ). The temporal robustness of NCEP-NCAR temperature at the interannual timescale is checked with the ERA-40 temperature reanalyses available until 2002 [Uppala *et al.*, 2005]. Over the 1965–2003 period, the mean seasonal NCEP-NCAR temperature variation is about  $9.4 \pm 1.5^\circ\text{C}$  that could explain a  $\delta^{18}\text{O}$  variation of  $4.0 \pm 0.6\text{‰}$  considering a slope of  $0.43\text{‰}/^\circ\text{C}$ . However, this estimate, applied for San Valentín summit, might be strongly underestimated because the  $\delta^{18}\text{O}/T$  slope increases with lower temperature due to a higher effective degree of rainout. We extract the high frequency from the isotopic signal using a MTM-SSA analysis, removing the first and the second principal components, i.e., the decadal trend, from the raw isotopic signal. The mean high frequency amplitude residual cycle is of  $5.3 \pm 2.2\text{‰}$  that could be mostly explained by the seasonal temperature variations assuming that the  $\delta/T$  gradient is actually of about  $0.6\text{‰}/^\circ\text{C}$ . Of course, this rough estimate does not account for possible isotopic diffusion affecting the seasonal cycle amplitude. At annual timescale, no correlation is found between isotopes and temperature even if (1) we consider only temperature during the rainiest months (April to September) and (2) we introduce some leads and lags in the dating without exceeding 5 years. The absence of correlation between  $\delta$  and temperature is also seen at the interannual timescale, when smoothing the signals from 5 to 11 years (Figure 5). Different processes could be invoked to account for this absence of relationship:

[50] (1) Atmospheric temperature reanalyses are averaged over a too large grid and do not represent the local surface temperature on the San Valentín summit area at interannual timescales [Garreaud *et al.*, 2008], (2) the isotopic composition does not account for temperature under a certain time resolution as it has been shown for Antarctica [Ekaykin *et al.*, 2002, 2004], (3) the isotopic composition of the firn is also related to other climate parameters as precipitation, moisture source changes (atmospheric circulation) or regional tropospheric temperature due to the high elevation location of the site, (4) as mentioned in section 2.4, because of wind erosion, part of the annual snow layer could be missing for specific years, leading to a seasonal bias when comparing the isotopic composition year-to-year (“summer” snow for one year could be compared to “winter” snow for another year). This last assumption, although not fully supported by calcium measurement (section 2.5), is interesting. Indeed, the highest interannual temperature variation over the 1965–2003 period from reanalyses is of  $2.3^\circ\text{C}$  and this is also what we observe in surrounding stations at lower latitude (at Puerto Aysen,  $45^\circ 24'\text{S}$ – $73^\circ 40'\text{W}$ , between 1965 and 1994, the highest interannual temperature variation is  $1.75^\circ\text{C}$  for an annual mean of  $8.8 \pm 0.5^\circ\text{C}$ , data from Dirección Meteorológica de Chile, J. Carrasco, personal communication) leading to a possible  $\delta^{18}\text{O}$  variation of about 1‰. However the firn core  $\delta^{18}\text{O}$  interannual variations range from  $-23.67$  to  $-10.48\text{‰}$  ( $m = -16.61\text{‰}$  and  $\sigma = 2.61$ ) with a strong low frequency of about 9.5 years (85% confidence level) and can attain  $\sim 8\text{‰}$  between 1986 and 1996 for example, leading to an interannual temperature change of about  $20^\circ\text{C}$  that is not realistic. The only one period when direct isotopic observations of precipitation and measurements on San Valentín

firn can be compared is between 1989 and 1998 when the isotopic composition of precipitation at Coyhaique varies within only 3‰, which is close to the 4‰ in the San Valentín firn over the same period. Regardless the origin of the 8‰-amplitude interannual shift in the San Valentín firn, it is worth noting that both sparse and short temperature measurements and tree-ring records from high elevation sites in Northern Patagonia indicate persistent and uncommon high temperatures in the 1980s referring to the last 250 years, in agreement with positive temperature anomalies in the tropical Pacific and along the western coast at about  $40^\circ\text{S}$  [Villalba *et al.*, 1997, 1998]. If higher temperatures in the middle of the 1980s by about 1 to  $2^\circ\text{C}$  cannot be a direct cause of the isotopic enrichment between 1980 and 1986, they could reflect regional climate changes possibly impacting the precipitation regime and snow deposition at San Valentín. For example, it has been shown that short and long term temperature variations at high elevation in northern Patagonia are mainly associated with forcing by the tropical oceans [Graham, 1995]. Thus further investigations will be required to understand mechanism linking the isotopic composition in San Valentín snow to the Pacific SST variability.

[51] We also seek for relationship between  $\delta$  and precipitation. However the comparison between GPCP (see section 1.2) and ERA-40 data sets from 1979 is definitely not robust at the interannual timescale both in amplitude and variation (not shown). Moreover, none of those two data sets can compare well with precipitation observations from Dirección Meteorológica de Chile. Thus, we are very doubtful about discussing here any comparison between isotopes and precipitation.

[52] At last, we would like to mention that no clear and consistent response can be observed between isotopic variations and specific ENSO events such as the strong El Niño events in 1972–73; 1982–83; 1986–87; 1992–93 or 1997–98 (Figure 5). However, considering the first half of the 1990s, when SOI is consistently negative, we find some high deuterium excess and low  $\delta^{18}\text{O}$  values that could be consistent with warmer oceanic sources and colder local temperatures ( $m_{1990-1995} = -18.13\text{‰}$ ,  $\sigma = 1.80$ ). Even though ENSO probably has an insignificant impact on temperature at this latitude [Rosenbluth *et al.*, 1997; Garreaud *et al.*, 2008], it is well known that positive phase of ENSO reduces precipitation by about 15%, over the west coast of Patagonia [Allan and D’Arrigo, 1999; Schneider and Gies, 2004] due to decreased westerly circulation. Precisely, it has been shown that the rainfall deficit occurs during summer (JFM) when El Niño attains its maximum. Thus, during El Niño years, the major part of the annual snow layer could be formed by winter precipitation falling during the cold season, and thus explaining the low isotopic composition. This process might be smoothed over our isotopic profile, except during the 1990–1995 period of persistent El Niño activity [Trenberth and Hoar, 1996; Allan and D’arrigo, 1999]. However strong changes in the rainfall at one season could impact the isotopic composition of precipitation because of precipitation seasonality changes, and thus we might expect to trace some strong ENSO events with a higher measurement resolution for isotopes. It is also worth noting that no correlation is found with the Antarctic

Oscillation (AAO, also known as the Southern Hemisphere Annular Mode) over the last 40 years (Figure 5). This is surprising as the AAO is known to have a significant impact on both surface air temperature [Garreaud *et al.*, 2008] and precipitation [Gillett *et al.*, 2006] in this region. Again, the isotopic composition of precipitation may be influenced by such a climate mode only on longer timescales.

### 3.2. Continental Influences

[53] In this section, the discussion is mainly focuses on  ${}_{\text{nss}}\text{Ca}^{2+}$  and nitrate.

#### 3.2.1. Dust From Erodible Soils

[54] The  ${}_{\text{nss}}\text{Ca}^{2+}$  profile as a record of soil dust mobilization and transport, and thus aridity and atmospheric circulation, has been extensively discussed in the dating section.  ${}_{\text{nss}}\text{Ca}^{2+}$  mean concentration at San Valentín ( $0.28 \pm 0.05 \mu\text{Eq. l}^{-1}$ ) is one order of magnitude lower than what is observed in tropical Andean sites that are very close to wide semi-arid sources ( $2.5 \pm 4.0 \mu\text{Eq. l}^{-1}$  along the Illimani ice core for a similar time period, [de Angelis *et al.*, 2003]). If one considers that precipitation carrying dust are not significantly removed by wind (see section 2.5), it makes sense to calculate annual values of  ${}_{\text{nss}}\text{Ca}^{2+}$  deposition flux. The  ${}_{\text{nss}}\text{Ca}^{2+}$  deposition flux (not shown) does not exhibit a large scattering with mean value of  $0.5 \pm 0.5 \text{ Eq. ha}^{-1} \text{ year}^{-1}$ , which is lower than the value of 3.8 calculated at Torres del Paine [Galloway *et al.*, 1996], a mid-latitude site at lower altitude on the eastern side of the Cordillera.  ${}_{\text{nss}}\text{Ca}^{2+}$  deposition flux higher than  $1 \text{ Eq. ha}^{-1} \text{ year}^{-1}$  (i.e., higher than the mean value plus the standard deviation, which denotes years with significantly more intense continental input) are observed in 1981, 1980 et 1975 (2.3, 2.8 and  $1.2 \text{ Eq. ha}^{-1} \text{ year}^{-1}$ , respectively). These higher values of  ${}_{\text{nss}}\text{Ca}^{2+}$  deposition flux are not related to any increase in calculated snow accumulation rate but to high concentration throughout the year. Interestingly, and as discussed in the following section, high nitrate and ammonium concentrations are also observed during these periods suggesting increased dust mobilization in relation with biomass burning events.

#### 3.2.2. Nitrate: A Tricky but Valuable Environmental Marker

[55] Associated with complementary indicators like  $\text{NH}_4^+$ , carboxylates, HCl and nonmarine  $\text{SO}_4^{2-}$ , nitrate is a key species to investigate changes in continental parameters: soil emission and thus temperature, rainfall and snow cover, biomass primary emission and fire events, fossil fuel burning and fertilization.

[56] In Figure 7, nitrate shows rather regular background variations often associated to similar trends of nonsea salt sulfate, although the amplitude of the variations of both species may be different. When sodium is low, such an apparent link may be due to the arrival of continental air masses influenced by combustion background. The presence of large amounts of nonmarine sulfate is supported by the profile of the ( $\text{MSA}/{}_{\text{nss}}\text{SO}_4^{2-}$ ) ratio (Figure 7) which shows marked decrease lasting several years, particularly in the deeper part of the core when sea salt input remains continuously low (1965–1983). This may be explained by a higher occurrence of air masses loaded with combustion products at San Valentín site during this period and/or by

higher emission rates leading to enhanced sulfate atmospheric background over a large part of South America. Complementary data of ammonium help to distinguish between biomass and fossil fuel burning. Three main periods of large biomass burning events may be identified (sulfate and nitrate peaks, no MSA, ammonium peaks and presence of mono and di-carboxylic acids): at 11.2 m (1975), around 9.7 m (1979–81) and around 4 m (1993–1994). Potential sources may be located eastward of the NPI, where widespread fires usually take place [Kitzberger *et al.*, 2001; Veblen and Kitzberger, 2002], but, as previously stated, occasional transport from Brazilian area may also occur. The largest event at 11.2 m, and dated in 1975 is presented in Figure 8. HCl peak, primary emission from biomass burning, is also clearly visible as well as a huge  ${}_{\text{nss}}\text{K}^+$  peak. During two of these three periods (1975, 1979–81) large amounts of calcium are also observed. This may be partly due to the strong convection associated to very high temperature in fire plumes leading to enhance the vertical mobilization of soil dust. Periods of sustained fire activity and high atmospheric dust load may also be related to precipitation deficiency over source areas, dryness increasing the amount of biomass fuel available for burning as well as soil erodibility.

[57] On the basis of the nitrate to sodium ratio during event B ( $0.02 \pm 0.01$ ) (see section 2.3), the part of nitrate which may be linked to marine primary aerosol is generally insignificant. Thus, when not associated to similar  ${}_{\text{nss}}\text{SO}_4^{2-}$  or  $\text{Na}^+$  spikes, nitrate increase can arise from higher lightning occurrence and/or polar vortex northward extension. Nitrate originating from the polar vortex and transported by polar marine air masses (see next section) seems a valuable hypothesis when nitrate levels correspond to high  $\text{Cl}_{\text{exc}}^-$  concentrations compared to the total  $\text{Cl}^-$  ones (2.5–3 m, 12–13 m and below 14.5 m).

[58] The comparison between nitrate and other chemical species concentrations clearly suggests that San Valentín summital area is strongly influenced by both continental and marine reservoirs. Their respective influence depends on the source strength but also on the alternance of specific climate modes at seasonal and interannual time scales. The amplitude and occurrence of marine inputs over the last 40 years are discussed in the following section, aiming to characterize the respective influences of continental and marine air masses origin.

### 3.3. Marine Inputs and Deuterium Excess: Complementary Markers of Atmospheric Circulation and Air masses Origin?

[59] Over remote ocean, a rapid decrease of marine primary aerosol with altitude is observed from the surface to about 1200 m [Shinozuka *et al.*, 2004]. Strong westerlies prevail most of the year in the Patagonian latitudinal belt leading to high sea salt production only partly counterbalanced by the increase of this vertical concentration gradient with increasing wind speed. Thus significant amounts of sea salt aerosol are expected to reach the inversion layer and act as cloud condensation nuclei while a smaller submicronic part reaches the free troposphere along with halogens and sulfur species [Von Glasow and Sander, 2002, Clarke and Kapustin, 2002]. The San Valentín summit area is less than 100 km away from the Pacific

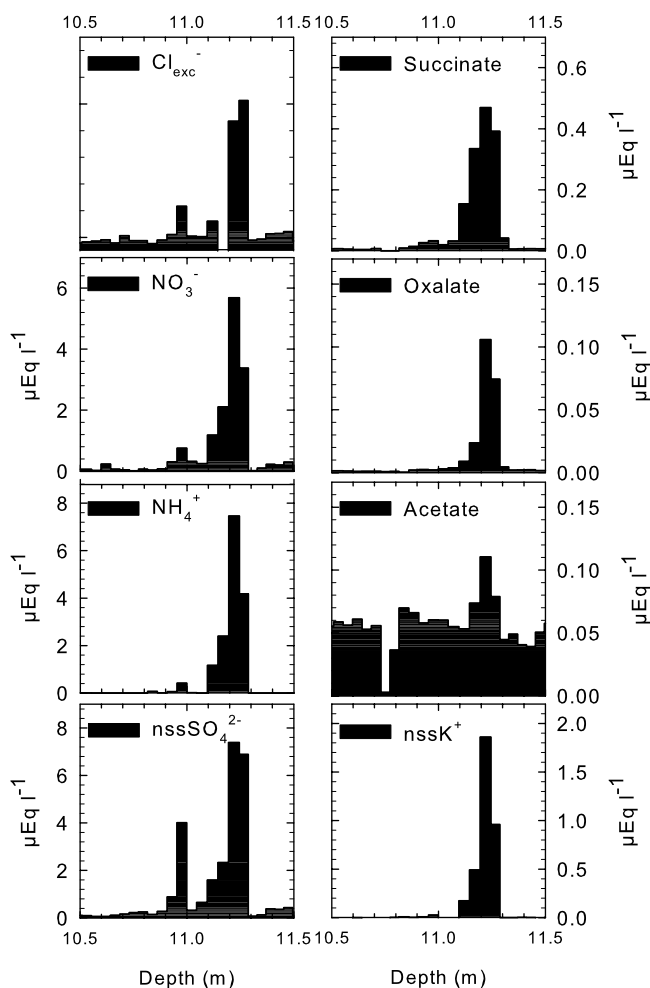


**Figure 8.** Selected chemical markers ( $\mu\text{Eq. l}^{-1}$ ) showing the occurrence of a large fire event dated in 1975.

Ocean coast and may be part of the year close to the top of the stratiform cloud coverage which controls the marine boundary layer during a large part of the year in southern South America as suggested by an ongoing and preliminary study aiming at estimating the elevation of the clouds layer relatively to the San Valentín summit using satellite pictures (F. Maignan, personal communication). Indeed, satellite pictures (MODIS) observed for each day of February and July 2001 show that, during austral winter, when a cloud layer is visible and originates from west, the San Valentín summit is fully covered. All that previous results lead us to expect a significant contribution of marine primary aerosol at the drilling site and allows us to use sodium as a valuable indicator of marine input, contrary to what occurs at tropical sites, located at higher altitude and where large sodium inputs observed during dry seasons are related to the arrival of continental halite [de Angelis *et al.*, 2003]. Considering the significant contribution of South American soils to San Valentín snow composition, any possible fingerprint of continental halite cannot be totally excluded. However sodium to chloride molar ratios measured along the entire profile ( $\text{Cl}/\text{Na}$  mean value = 1.137,  $\sigma = 0.008$ ) are very close to the bulk sea water value of 1.169 [Keene *et al.*, 1986] i.e., higher than in halite, which is another argument

for considering that  $\text{Cl}^-$  and  $\text{Na}^+$  are mainly of marine origin at the San Valentín site.

[60] The sodium profile (Figure 9) exhibits huge temporal variations with several wide background increases lasting a few years and superimposed on thinner relative maxima between 1984 and 1996 (from  $\sim 4.5$  to 8 m) and in 2004–2005 (the first upper 50 cm). On the contrary, very low values prevail from the late 1960s to the early 1980s and between 1998 and 2004. Except the large peak centered at 5 m depth and likely corresponding to volcanic halite, sodium concentrations do not exceed 10 to 20  $\mu\text{Eq. l}^{-1}$  which is close to what is observed in Antarctic snow at an elevation of 1000 m and 200–300 km far from the coast [Wagenbach *et al.*, 1998]. Excess of chloride ( $\text{Cl}_{\text{exc}}^-$ ) (Figure 7), with respect to bulk sea water composition, is used to estimate the marine primary aerosol alteration through heterogeneous chemical processes occurring within the marine boundary layer or inside clouds. A slight deficit of chloride (negative values of  $\text{Cl}_{\text{exc}}^-$ ), representing a few percent of total chloride, is systematically observed when marine input is strong. This is not surprising, since wet heterogeneous chemical processes occurring in marine environment lead to interaction between marine primary aerosol (dominated by NaCl) and acidic gases, in particular  $\text{SO}_2$ . Because of acid attack, HCl is formed and escapes from marine aerosol, so that the marine aerosol becomes Cl depleted, Cl losses increasing from a few percents up to several tens of percents as aerosol ages. Slight deficit of chloride indicates [Ikegami *et al.*, 1994] that rapid transport from oceanic sources by prevailing western winds prevent marine salts from being significantly modified by atmospheric oxidation processes. The profile of methanesulfonate (MSA) (Figure 9), a sulphur oxidation product of marine biogenic origin, matches closely the sodium profile. Although MSA formation depends on chlorophyll and biomass location which may be different from the primary aerosol production area, and despite lower vertical concentration gradient for sulfur species compared to marine salts, exchange between air masses transporting marine primary or secondary aerosols are expected along zonal eastward trajectories. All together, these results demonstrate that large amounts of marine aerosols are transported to San Valentín. Stronger events are observed at pluri-annual timescale and may be related to changes in Southern Hemisphere tropospheric main features. Such changes include both the South Pacific anticyclone position and strength and the Southern Hemisphere annular mode, possibly impacting as far south as Northern Patagonia [Aceituno, 1989; Thompson and Solomon, 2002]. When the marine input is weaker (from  $\sim 1$  to 3 m and in the deeper part of the core),  $\text{Cl}_{\text{exc}}^-$  becomes positive and varies between 20 and 50% of total  $\text{Cl}^-$ , which is significant since the analytical uncertainty varies from  $\sim 10\%$  for  $\text{Cl}_{\text{exc}}^- > 0.05 \mu\text{Eq. l}^{-1}$  to  $\sim 60\%$  when  $\text{Cl}_{\text{exc}}^-$  decreases below  $0.02 \mu\text{Eq. l}^{-1}$ . This indicates the presence of HCl and thus a more efficient oxidation of marine aerosol during transport that could be due to a higher aerosol surface to volume ratio, aging processes of air masses and/or to a greater relative abundance of  $\text{SO}_2$ , N gases and oxidizing species. This also supports the assumption that marine aerosols are larger (smaller) and directly transported by west winds (transported by aged air masses) during periods of high (low) marine inputs. However, most of HCl occurrences are well correlated with nitrate occurrences as clearly

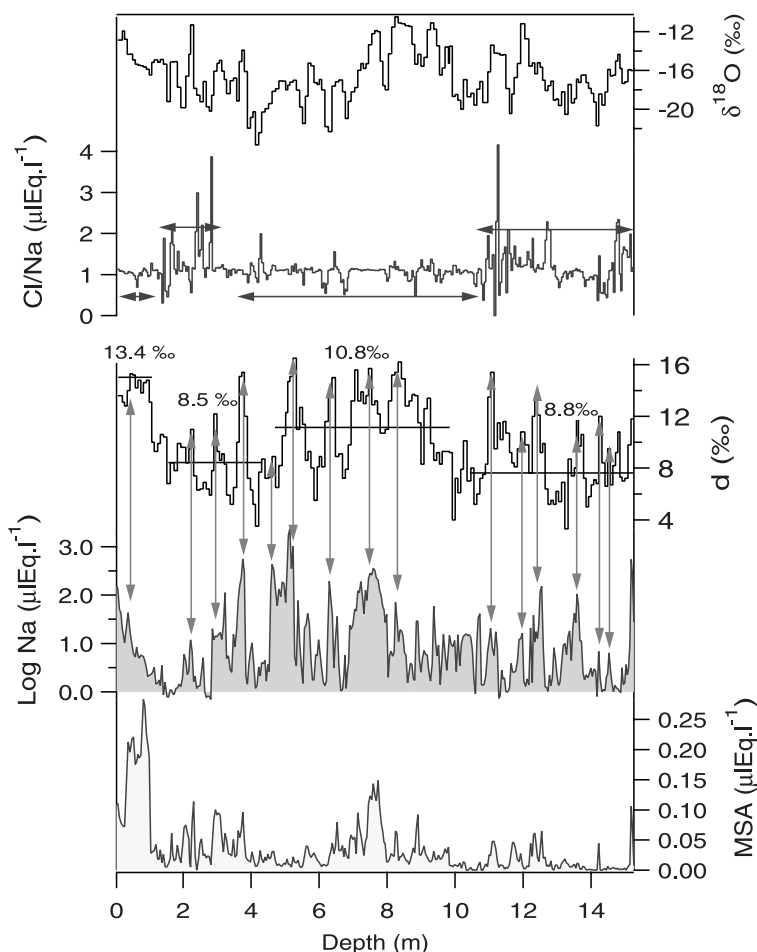


**Figure 9.** Selected chemical markers of marine inputs ( $\mu\text{Eq. l}^{-1}$ ),  $\delta^{18}\text{O}$  and deuterium excess of the ice ( $\text{‰}$ ). Vertical arrows indicate similar occurrences in sodium concentration and deuterium excess.

shown in Figure 7. Considering the possible nitrate sources (see previous section), this correlation during periods of lower marine inputs may indicate that HCl has partly a non-marine origin [beside its component related to combustions, HCl is for instance a primary emission of road transport in the agricultural-industrial region of South America, *da Rocha et al.*, 2003] and is entrapped in marine air masses overflying the continent along a NE-SW direction. This may occur when the cloud cover shifts northward in winter, allowing continental air masses to reach mid latitudes along the eastern side of the Andes [*Diaz et al.*, 2006]. On the other hand, nitrate sedimenting from stratospheric sources like polar stratospheric clouds or originating from the long range transport of peroxyacetyl nitrate (PAN, a pollutant sufficiently stable under conditions of low temperature and low  $[\text{NO}]/[\text{NO}_2]$  ratios prevailing in winter at high latitude Southern Pacific [see for instance *Singh et al.*, 1985]) may have been mixed with old marine air masses flying close to the polar vortex.

[61] Despite the different sampling resolution, we observe that deuterium excess is lower when Cl/Na ratio is scattered and often high (Figure 9) and sodium concentrations are low. Deuterium excess is lower between 1.2 and 2.8 m and below 10.8 m (between 1997 and 2001 and before 1977) with a mean value of 8.7‰ and a standard deviation of

2.3‰. During these periods, the Cl to Na ratio is generally significantly higher than the marine reference and sodium concentrations are low which suggests the arrival of fine aged marine aerosol transported by aged airmasses. Thus periods of low deuterium excess could reflect a polar origin for precipitation [in polar areas, deuterium excess is a positive proxy of moisture source temperature, *Vimeux et al.*, 1999] whereas periods of high deuterium excess corresponding to a Cl/Na ratio close to the bulk sea water value and high level of Na (Na peaks match maxima of deuterium excess), may indicate warmer moisture source and direct moisture transport from the Pacific Ocean. This latter pattern is observed between 0 and 1.1 m (after 2001) and between 2.9 and 10.8 m depth (1976–1997), with a mean deuterium excess value of 10.7‰ and a standard deviation of 3.2‰ (although some matches exist also below 10.8 m and between 1.2 and 2.8 m). Interestingly, a fair match seems to exist over the whole profile between peaks of deuterium excess and (1) sodium at a higher frequency (see arrows in Figure 9) and (2) the marine biogenic productivity tracked by MSA, a marine biogenic input indicator. The existence of two very distinct climate modes for humidity suggested by our data requires further investigation even if it is supported by backtrajectories calculated for present-day at different seasons (HYSPLIT model,

<http://www.arl.noaa.gov/ready.html>) which clearly show that these two origins (Polar versus Pacific Ocean) exist. Actually, we assume here that (1) same air masses bring part of precipitation and marine aerosols at the interannual timescale over the San Valentín area whereas deposition/accumulation processes for both precipitation and aerosol need to be investigated and (2) deuterium excess is a proxy of moisture source temperature as in Antarctica.

#### 4. Conclusion and Perspectives

[62] For the first time in this paper, a  $\sim 40$ -year-long paleoclimate and paleoenvironmental record from Patagonian ice unperturbed by water percolation and with no missing year is presented. The mean snow accumulation rate estimated from the combination of several indicators, is around  $36 \pm 3$  cm of snow per year. It appears very low compared to lower altitude sites. That may be related both to the moisture gradient over the Patagonian Andes and to fresh snow redistribution by wind erosion during storm events although no missing year appears in the dating.

[63] Comparison of isotopic and chemical profiles suggests that the San Valentín area alternatively undergoes two kinds of influences, the relative importance of which varying at interannual timescale: the site is influenced by air masses originating from the South Pacific and rapidly transported by western winds, but a second very different mode, corresponding to air masses overflying the continent through a N–NE circulation pattern with combustion events, erodible soils, and biomass emission signatures, is also observed. The later one may be mixed with aged marine air masses of polar origin. Therefore, our results indicate that precipitation at that site is not controlled the whole-year long by westerlies and that meteorological patterns allowing aerosol and gas transport from eastern Patagonia and even Brazil regularly occur which is an unexpected results.

[64] On the basis of this detailed and promising study, a deep ice core (122 m) and several shallow firn cores (from 20 to 70 m) were drilled to the bedrock in May 2007, very close to the 2005 drilling site. They should provide information on the natural variability of aridity, biomass emission, ocean productivity and cyclogenesis at mid latitudes of the Southern Hemisphere and allow us to reconstruct climate and environmental variations at high resolution through the entire Holocene in relation with anthropic influence and what is known for lower (tropical) and higher (polar) latitude areas. To interpret those future records, a special attention will have to be done on the understanding on the isotopic proxies in relation with the main climate modes in that region (SAM-AOO, ENSO). A longer isotopic record could also offer the possibility to reduce the remaining uncertainties on the  $\delta$ -climate relationship.

[65] **Acknowledgments.** We deeply thank Ulrich Schotterer for the Tritium measurement in the deepest samples. We also thank Frédéric Chevallier, Sandrine Bony, and Paulina Lopez for their help in accessing the NCEP-NCAR and ERA-40 reanalyses and the GPCP data set, and Fabienne Maignan for preliminary discussions on satellite pictures. This paper has been improved by discussions with Valérie Masson-Delmotte, Georg Hoffmann and Pierre-Alain Danis and by comments from three anonymous reviewers. The March 2005 field campaign and the analyses of the firn core were funded by IRD, LSCE (CEA-CNRS-UVSQ) and LGGE (CNRS-UJF). Logistic support from Carabineros de Chile is gratefully acknowledged. Alejandro Colomé collaborated with cold storage of the

firn core in Coyhaique. G.C. was sponsored by Fondo Nacional de Ciencia y Tecnología de Chile (FONDECYT 1040989 and 1061269) and Centro de Estudios Científicos (CECS). CECS is funded by the Millennium Science Initiative and grants from Empresas CMPC, Andes and Tinker Foundations.

#### References

- Aceituno, P. (1989), On the functioning of the Southern Oscillation in the South American sector, Part II: Upper-air circulation, *J. Clim.*, *21*, 341–355.
- Adler, R., et al. (2003), The Version-2 Global Precipitation Climatology Project (GPCP) monthly precipitation analysis (1979–present), *J. Hydro-meteor.*, *4*, 1147–1167.
- Allan, R. J., and R. D. D'Arrigo (1999), "Persistent" ENSO sequences: How unusual was the 1990–1995 El Niño?, *Holocene*, *9*, 101–118.
- Appleby, P. G., N. Richardson, and P. J. Nolan (1991),  $^{241}\text{Am}$  dating of lake sediments, *Hydrobiologia*, *214*, 35–42.
- Aristarain, A. J., and R. J. Delmas (1993), Firn-core study from the southern Patagonia ice cap, South America, *J. Glaciol.*, *39*, 249–254.
- Arnaud, F., O. Magand, E. Chapron, S. Bertrand, X. Boes, F. Charlet, and M. A. Melières (2006), Radionuclide dating ( $^{210}\text{Pb}$ ,  $^{137}\text{Cs}$ ,  $^{241}\text{Am}$ ) of recent lake sediments in a highly active geodynamic setting (Lakes Puyhue and Icalma-Chilean Lake District), *Sci. Total Environ.*, *366*, 837–850.
- Blindow, N., and F. Thyssen (1986), Ice thickness and inner structure of the Vernagtferner (Oetztal Alps): Results of electromagnetic reflection measurements, *Zeitschrift Gletscherkunde Glazialgeologie*, *22*, 43–60.
- Bull, C. (1971), Snow accumulation in Antarctica, *Publ. Am. Assoc. Adv. Sci.*, 367–421.
- Carrasco, J., G. Casassa, and A. Rivera (2002), Meteorological and climatological aspects of the Southern Patagonia ice cap, Patagonia, in *The Patagonian Icefields: A Unique Natural Laboratory for Environmental and Climate Change Studies*, edited by G. Casassa, F. Sepúlveda, and R. Sinclair, pp. 29–41, Kluwer Academic/Plenum Publishers, New York.
- Casassa, G., and A. Rivera (1998), Digital radio-echo sounding at Tyndall Glacier, Patagonia, *Anales Instituto Patagonia, Serie Cienc. Nat. (Chile)*, *26*, 129–135.
- Clarke, A. D., and V. N. Kapustin (2002), A Pacific Aerosol Survey. Part I: A decade of data on particle production, transport, evolution and mixing in the troposphere, *J. Atmos. Sci.*, *59*, 363–382.
- Dansgaard, W. (1964), Stable isotopes in precipitation, *Tellus*, 436–447.
- Da Rocha, G. O., A. Franco, A. G. Allen, and A. A. Cardoso (2003), Source of atmospheric acidity in an agricultural-industrial region of São Paulo State, Brazil, *J. Geophys. Res.*, *108*(D7), 4207, doi:10.1029/2002JD002567.
- De Angelis, M., and M. Legrand (1995), Origins and variations of light carboxylic acids in polar precipitation., *J. Geophys. Res.*, *100*(D1), 1445–1462.
- De Angelis, M., J. P. Steffensen, M. Legrand, H. B. Clausen, and C. U. Hammer (1997), Primary aerosol (sea salt and soil dust) deposited in Greenland ice during the last climatic cycle: Comparison with east Antarctic records, *J. Geophys. Res.*, *102*(C12), 26,681–26,698.
- De Angelis, M., J. C. Simões, H. Bonnaveira, D.-J. Taupin, and R. Delmas (2003), Volcanic eruptions recorded in the Illimani ice core (Bolivia): 1918–1998 and Tambora periods, *Atmos. Chem. Phys.*, *3*, 1725–1741.
- Delmas, R., and M. Pourchet (1977), Utilisation des filtres échangeurs d'ions pour l'étude de l'activité  $\beta$  globale d'un carottage glaciologique, *IAHS Publ.*, *118*, 159–163.
- Delmelle, P., M. Lambert, Y. Dufrière, P. Gerin, and N. Oskarsson (2007), Gas/aerosol–ash interaction in volcanic plumes: New insights from surface analysis of fine ash particles, *Earth Planet. Sci. Lett.*, *259*, 159–170.
- Diaz, S., et al. (2006), Ozone and UV radiation over South America: Climatology and anomalies, *Photochem. Photobiol.*, *B2*, 834–843.
- Eisenbud, M., and T. Gesell (Eds.) (1997), *Environmental Radioactivity From Natural, Industrial and Military Sources*, 4th ed., San Diego Academic Press, San Diego.
- Eisen, O., et al. (2008), Ground-based measurements of spatial and temporal variability of snow accumulation in East Antarctica, *Rev. Geophys.*, doi:10.1029/2006RG000218, in press.
- Ekaykin, A. A., V. Y. Lipenkov, N. I. Barkov, J. R. Petit, and V. Masson-Delmotte (2002), Spatial and temporal variability in isotope composition of recent snow in the vicinity of Vostok Station: implications for ice-core record interpretation, *Ann. Glaciol.*, *35*, 181–186.
- Ekaykin, A., V. Lipenkov, I. Kuzmina, J. R. Petit, V. Masson-Delmotte, and S. J. Johnsen (2004), The changes in isotope composition and accumulation of snow at Vostok station, East Antarctica, over the past 200 years, *Ann. Glaciol.*, *39*, 569–575.
- EPICA community members (2004), Eight glacial cycles from an Antarctic ice core, *Nature*, *429*, 623–628.
- Fricke, H. C., and J. R. O'Neil (1999), The correlation between  $^{18}\text{O}/^{16}\text{O}$  ratios of meteoric water and surface temperature: Its use in investigating

- terrestrial climate change over geologic time, *Earth Planet. Sci. Lett.*, **170**, 181–196.
- Galloway, J. N., W. C. Keene, and G. E. Likens (1996), Processes controlling the composition of precipitation at a remote southern hemispheric location: Torres del Paine National Park, Chile, *J. Geophys. Res.*, **101**(D3), 6883–6897.
- Garreaud, R., M. Vuille, R. Compagnucci, and J. Marengo (2008), Present-day South American Climate, *Palaeogeogr. Palaeoclimatol. Palaeoecol.*, in press.
- Gillett, N. P., T. D. Kell, and P. D. Jones (2006), Regional climate impacts of the Southern Annular Mode, *Geophys. Res. Lett.*, **33**, L23704, doi:10.1029/2006GL027721.
- Ginot, P., F. Stampfli, D. Stampfli, M. Schwikowski, and H. W. Gäggeler (2002), FELICS, a new ice core drilling system for high-altitude glaciers, *Mem. Natl. Inst. Polar Res., Spec. Issue*, **56**, 38–48.
- Goldberg, E. D. (1963), Geochronology with Lead-210, in *Radioactive Dating, Proceedings of a Symposium*, edited by IAEA and ICSU, pp. 121–131, Vienna.
- Graham, N. E. (1995), Simulation of recent global temperature trends, *Science*, **267**, 666–671.
- Hoffmann, G., M. Werner, and M. Heimann (1998), The water isotope module of the ECHAM atmospheric general circulation model: A study on time scales from days to several years, *J. Geophys. Res.*, **103**(D14), 16,871–16,896.
- Ichiyanagi, K., A. Numaguti, and K. Kato (2002), Interannual variations of stable isotopes in Antarctic precipitation in response to El Niño Southern Oscillation, *Geophys. Res. Lett.*, **29**(1), 1001, doi:10.1029/2000GL012815.
- Ikegami, M., K. Okada, Y. Zaizen, and Y. Makino (1994), Sea-salt particles in the upper tropical troposphere, *Tellus*, **46B**, 142–151.
- Instituto Geográfico Militar (Chile) (1982), Carta Monte San Valentín o San Clemente, 1: 50,000, 132.
- Inoue, J., H. Kondo, Y. Fujikoshi, T. Yamada, H. Fukami, and C. Nakajima (1987), Summer climate of the Northern Patagonia Icefield, *Bull. Glacier Res.*, **4**, 7–14.
- Johnsen, S., and G. Q. Robin (1983), Diffusion of stable isotopes, in *The Climatic Record in Polar Ice Sheets*, edited by G. Q. Robin, pp. 57–63, Cambridge Univ. Press, New York.
- Kalnay, E., et al. (1996), The NCEP/NCAR 40-year reanalysis project, *Bull. Am. Meteorol. Soc.*, **7**, 437–471.
- Keene, W., A. Pszenny, J. Galloway, and M. Hawley (1986), Sea-salt corrections and interpretation of constituent ratios in marine precipitation, *J. Geophys. Res.*, **91**(D6), 6647–6658.
- Kitzberger, T., T. W. Swetnam, and T. T. Veblen (2001), Inter-hemispheric synchrony of forest fires and the El Niño-Southern Oscillation, *Global Ecol. Biogeogr.*, **10**, 315–326.
- Krishnaswami, D., J. M. Lal, M. Martin, and M. Meybeck (1971), Geochronology of lake sediments, *Earth Planet. Sci. Lett.*, **11**, 407–414.
- Labraga, J. C. (1994), Extreme winds in the Pampa del Castillo Plateau, Patagonia, Argentina, with reference to Wind Farm Settlement, *J. Appl. Meteorol.*, **33**, 85–95.
- Lamy, F., D. Hebbeln, U. Rohl, and G. Wefer (2001), Holocene rainfall variability in southern Chile: A marine record of latitudinal shifts of the Southern Westerlies, *Earth Planet. Sci. Lett.*, **185**, 369–382.
- Magand, O., and F. Arnaud (2007), Response on the comment from Ribeiro Guevara and Arribere on the article “Radionuclide profiles (Pb-210, Cs-137, Am-241) of recent lake sediments in a highly geodynamic settings (Lakes Puyehue and Icalma-Chilean Lake District)”, *Sci. Total Environ.*, **385**, 312–314, doi:10.1016/j.scitotenv.2007.05.022.
- Mann, M. E., and J. M. Lees (1996), Robust estimation of background noise and signal detection in climatic series, *Clim. Change*, **33**, 409–445.
- Matsuoka, K., and R. Naruse (1999), Mass balance features derived from a firn core at Hielo Patagonico Norte, South America, *Arct. Antarct. Alpine Res.*, **31**, 333–340.
- Moxey, L. E. (2004), Mount Hudson’s 1991 eruption provides Holocene paleoclimatic insights, *Int. J. Remote Sens.*, **25**(6), 1053–1062.
- Naranjo, J. A., H. Moreno, and N. Banks (1993), La erupción Volcán Hudson en 1991 (46°S) Región XI, Aisén, Chile, *Bol. Serv. Nac. Geol. Min. Chile*, **44**, 1–50.
- Oldfield, F., N. Richardson, and P. G. Appleby (1995), Radiometric dating (<sup>210</sup>Pb, <sup>137</sup>Cs, <sup>241</sup>Am) of recent ombrotrophic peat accumulation and evidence for changes in mass balance, *Holocene*, **5**, 141–148.
- Paruelo, J. M., A. Beltran, E. Jobbágy, O. E. Sala, and R. A. Golluscio (1998), The climate of Patagonia: General patterns and controls on biotic processes, *Ecologia Austral.*, **8**, 85–101.
- Pereira, E. B., H. E. Evangelista, K. C. Dalia Pereira, I. F. A. Cavalcanti, and A. W. Setzer (2006), Apportionment of black carbon in the South Shetland Islands, Antarctic Peninsula, *J. Geophys. Res.*, **111**, D03303, doi:10.1029/2005JD006086.
- Popovnin, V. V., T. A. Danilova, and D. A. Petrakov (1999), A pioneer mass balance estimate for a Patagonian glacier: Glaciar De los Tres, Argentina, *Global Planet. Change*, **22**, 255–267.
- Pourchet, M., O. Magand, M. Frezzotti, A. A. Ekaykin, and J. G. Winter (2003), Radionuclides deposition over Antarctica, *J. Environ. Radioact.*, **68**, 137–158.
- Preiss, N., M. A. Mélières, and M. Pourchet (1996), A compilation of data on lead 210 concentration in surface air and fluxes at the air-surface and water-sediment interfaces, *J. Geophys. Res.*, **101**(D22), 28,847–28,862.
- Prospero, J. M., P. Ginoux, O. Torres, and S. E. Nicholson (2002), Environmental characterization of global sources of atmospheric soil dust derived from the NIMBUS-7 TOMS absorbing aerosol product, *Rev. Geophys.*, **40**(1), 1002, doi:10.1029/2000RG000095.
- Ramirez, E., et al. (2003), A new Andean deep ice core from Nevado Ilimani, 6350 m, Bolivia, *Earth Planet. Sci. Lett.*, **212**, 337–350.
- Ribeiro Guevara, S., A. Rizzo, R. Sanchez, and M. Arribere (2003), <sup>210</sup>Pb fluxes in sediment layers sampled from Northern Patagonia lakes, *J. Radioanal. Nucl. Chem.*, **258**(3), 583–595.
- Rivera, A., T. Benham, G. Casassa, J. Bamber, and J. Dowdeswell (2007), Ice elevation and areal changes of glaciers from the Northern Patagonia icefield, Chile, *Global Planet. Change*, **59**, 126–137.
- Rosanski, K., L. Araguas-Araguas, and R. Gonfiantini (1993), Isotopic patterns in modern global precipitation, in *Climate Change in Continental Isotopic Records*, *Geophys. Monogr. Ser.*, vol. 78, pp. 1–37, AGU, Washington D.C.
- Rose, W. I., G. J. S. Bluth, and G. G. Ernst (2000), Integrating retrievals of volcanic cloud characteristics from satellite remote sensors: A summary, *Phil. Trans. R. Soc. London Ser. A*, **358**, 1585–1606.
- Rosenbluth, B., H. A. Fuenzalida, and P. Aceituno (1997), Recent temperature variations in southern South America, *Int. J. Climatol.*, **17**, 67–85.
- Schneider, C., and D. Gies (2004), Effects of El Niño-Southern Oscillation on southernmost South America precipitation at 53°S revealed from NCEP-NCAR reanalyses and weather station data, *Int. J. Climatol.*, **24**, 1057–1076.
- Schneider, C., M. Glaser, R. Kilian, A. Santana, N. Butorovic, and G. Casassa (2003), Weather observations across the southern Andes at 53°S, *Phys. Geogr.*, **24**, 97–119.
- Schwikowski, M., S. Brütsch, G. Casassa, and A. Rivera (2006), A potential high-elevation ice-core site at Hielo Patagónico Sur, *Ann. Glaciol.*, **43**, 8–13.
- Shinozuka, Y., A. D. Clarke, S. G. Howell, V. N. Kapustin, and B. J. Huebert (2004), Sea-salt vertical profiles over the Southern and tropical Pacific oceans: Microphysics, optical properties, spatial variability, and variations with wind speed, *J. Geophys. Res.*, **109**, D24201, doi:10.1029/2004JD004975.
- Shiraiwa, T., S. Kohshima, R. Uemura, N. Yoshida, S. Matoba, J. Uetake, and M. A. Godoi (2002), High net accumulation rates at Campo de Hielo Patagonico Sur, South America, revealed by analysis of a 45.97m long ice core, *Ann. Glaciol.*, **35**, 84–90.
- Singh, H. B., L. J. Salas, B. A. Ridley, J. D. Shetter, N. M. Donahue, F. C. Fehsenheld, D. W. Fahey, D. D. Parrish, and E. J. Williams (1985), Relationship between peroxyacetyl nitrate and nitrogen oxides in the clean troposphere, *Nature*, **318**, 347–349.
- Smellie, J. L. (1999), The upper Cenozoic tephra record in the south polar region: A review, *Global Planet. Change*, **21**, 51–70.
- Smith, J. T. (2001), Why should we believe <sup>210</sup>Pb sediment geochronologies?, *J. Environ. Radioact.*, **55**, 121–123.
- Stoiber, R. E., and W. I. Rose Jr. (1974), Fumarole incrustation of active Central American volcanoes, *Geochim. Cosmochim. Acta*, **38**, 495–516.
- Thompson, D. W. J., and S. Solomon (2002), Interpretation of recent Southern Hemisphere climate change, *Science*, **296**, 895–899.
- Thompson, L. G., E. Mosley-Thompson, and K. A. Henderson (2000), Ice-core palaeoclimate records in tropical South America since the last glacial maximum, *J. Quaternary Sci.*, **15**, 377–394.
- Thompson, L. G., E. Mosley-Thompson, M. E. Davis, P. N. Lin, K. Henderson, and T. A. Mashiotta (2003), Tropical glacier and ice core evidence of climate change on annual to millennial time scales, *Clim. Change*, **59**, 137–155.
- Trenberth, K. E., and T. J. Hoar (1996), The 1990–1995 El Niño-Southern oscillation event: Longest on record, *Geophys. Res. Lett.*, **23**, 57–60.
- Uppala, S. M., et al. (2005), The ERA-40 reanalysis, *Q. J. R. Meteorol. Soc.*, **131**, 2961–3012.
- Veblen, T. T., and T. Kitzberger (2002), Inter-hemispheric comparison of fire history: The Colorado Front Range, U.S.A., and the Northern Patagonian Andes, Argentina, *Plant Ecol.*, **163**, 187–207.
- Villalba, R., J. A. Bonnisegna, T. T. Veblen, A. Schmelter, and S. Rubulis (1997), Recent trends in tree-ring records from high elevation sites in the Andes of Northern Patagonia, *Clim. Change*, **36**, 425–454.

- Villalba, R., E. R. Cook, G. C. Jacoby, R. D. D'Arrigo, T. T. Veblen, and P. D. Jones (1998), Tree-ring based reconstructions of Northern Patagonia precipitation since AD 1600, *Holocene*, 8, 659–674.
- Villalba, R., A. Lara, J. A. Boninsegna, M. Masiokas, S. Delgado, J. C. Aravena, F. A. Roig, A. Schmelter, A. Wolodarsky, and A. Ripalta (2003), Large-scale temperature changes across the Southern Andes: 20th-century variations in the context of the past 400 years, *Clim. Change*, 59, 177–232.
- Vimeux, F., V. Masson, J. Jouzel, M. Stievenard, and J. R. Petit (1999), Glacial–interglacial changes in ocean surface conditions in the Southern Hemisphere, *Nature*, 398, 410–413.
- Von Glasow, R., and R. Sander (2002), Modelling halogen chemistry in the marine boundary layer 1. Cloud-free MBL, *J. Geophys. Res.*, 107(D17), 4341, doi:10.1029/2001JD000942.
- Wagenbach, D., F. Ducroz, R. Mulvaney, L. Keck, A. Minikin, M. Legrand, J. S. Hall, and E. Wolff (1998), Sea-salt aerosol in coastal Antarctic regions, *J. Geophys. Res.*, 103(D9), 10,961–10,974.
- Werner, M., and M. Heimann (2002), Modelling interannual variability of water isotopes in Greenland and Antarctica, *J. Geophys. Res.*, 107(D1), 4001, doi:10.1029/2001JD900253.
- Witham, C. S., C. Oppenheimer, and C. J. Horwell (2005), Volcanic ash-leachates: A review and recommendations for sampling methods, *J. Volcanol.*, 141, 299–326.
- Wolff, E., et al. (2006), Southern Ocean sea-ice extent, productivity and iron flux over the past eight glacial cycles, *Nature*, 440, 491–496.
- Woods, D. C., R. L. Chuan, and W. I. Rose (1985), Halite particles injected into the stratosphere by the 1982 El Chichón eruption, *Science*, 230, 170–172.
- Yamada, T. (1987), Glaciological characteristics revealed by 37.6-m deep ice core drilled at the accumulation area of San Rafael Glacier, the Northern Patagonian Icefield, *Bull. Glacier Res.*, 4, 59–67.
- 
- G. Casassa, CECS, Centro de Estudios Científicos, Av. Prat 514, Valdivia, Chile.
- M. de Angelis and O. Magand, LGGE, Laboratoire de Glaciologie et Géophysique de l'Environnement, CNRS, Université Joseph Fourier-Grenoble, 54 rue Molière, BP 96, 38402 Saint Martin d'Hères, Cedex, France.
- S. Falourd, LSCE, CE Saclay, Orme des Merisiers, Bat. 701, 91191, Gif-sur-Yvette Cedex, France.
- P. Ginot, IRD, UR Great Ice, IHH, 9214, La Paz, Bolivia.
- S. Johnsen, Department of Geophysics, University of Copenhagen, Juliane Maries Vej 30, DK-2100, Copenhagen, Denmark.
- B. Pouyaud, IRD, Institut de Recherche pour le Développement, UR Great Ice, MSE, 34095, Montpellier Cedex 5, France.
- F. Vimeux, IRD, UR Great Ice, LSCE, CE Saclay, Orme des Merisiers, Bat. 701, 91191, Gif-sur-Yvette Cedex, France. (francoise.vimeux@lsce.ipsl.fr)